# On the Use of Exponential Basis Functions in the Analysis of Shear Deformable Laminated Plates

M. Shahbazi
B. Boroomand
S. Soghrati

Publication CIMNE Nº-353, February 2011

# On the Use of Exponential Basis Functions in the Analysis of Shear Deformable Laminated Plates

M. Shahbazi
B. Boroomand
S. Soghrati

**Publication CIMNE Nº-353, February 2011**

**International Center for Numerical Methods in Engineering**
Gran Capitán s/n, 08034 Barcelona, Spain

# On the Use of Exponential Basis Functions in the Analysis of Shear Deformable Laminated Plates

M. Shahbazi[1], B. Boroomand[2], S. Soghrati [3]

[1,2] *Department of Civil Engineering, Isfahan University of Technology, Isfahan 84156-83111, Iran*
*E-mail: Boromand@cc.iut.ac.ir*

[3] *Department of Civil and Environmental Engineering, University of Illinois at Urbana-Champaign, 205 North Mathews Avenue, Urbana, II, 61801, USA*

## Abstract

In this report, we introduce a meshfree approach for static analysis of isotropic/orthotropic cross-ply laminated plates with symmetric/non-symmetric layers. Classical, first and third order shear deformation plate theories are employed to perform the analyses. In this method, the solution is first split into homogenous and particular parts and then the homogenous part is approximated by the summation of an appropriately selected set of exponential basis functions (EBFs) with unknown coefficients. In the homogenous solution the EBFs are restricted to satisfy the governing differential equation. The particular solution is derived using a similar approach and another series of EBFs. The imposition of the boundary conditions and determination of the unknown coefficients are performed by a collocation method through a discrete transformation technique. The solution method allows us to obtain semi-analytical solution of plate problems with various shapes and boundary conditions. The solutions of several benchmark plate problems with various geometries are presented to validate the results.

**Keywords:** *Meshfree, Laminated plate, Classical plate theory, Shear deformation plate theories, Exponential basis function, Discrete transformation*

[1] Graduate Student
[2] Professor
[3] Ph.D. Candidate

## Contents

# 1. INTRODUCTION

The wide application of moderately thick and thin plates in structural components has turned the bending analysis of plates into one of the most important engineering concerns. For this purpose, several plate theories have been developed to address this problem. The classical plate theory (CLPT) based on the Kirchhoff's assumptions (1850), in which the straight lines normal to the mid-plane remain straight and normal after the deformation, disregards the effect of transverse shear strains. This leads to underestimation of the deflections and overestimations of natural frequencies and critical loads especially in plates with high thickness-to-length ratios. These errors are even more pronounced in laminated plates made of fiber reinforced composites with high elastic modulus to shear modulus ratios. In order to account for the influence of the transverse shear deformations on the bending deformations, a category of plate theories known as the shear deformation theories have been introduced in the literature.

Mindlin (1951) proposed the first order shear deformation theory (FSDT), in which the transverse shear strains and stresses are assumed to be constant across the thickness of the plate. This theory requires a shear correction factor to compensate its inability in satisfying the zero-traction boundary conditions on the top and bottom surfaces of the plate. Several higher order shear deformation theories (HSDT) (Whitney and Sun, 1974; Lo et al., 1977; Levinson, 1980; Reddy, 1984), assuming a Taylor expansion of the in-plane displacements in terms of the plate thickness coordinate, have been proposed to overcome the FSDT deficiencies. Among the higher order theories the third order shear deformation theories (TSDT) developed by Levinson (1980) and Reddy (1984) are the most prevalent ones in the analysis of laminated plates.

Exact analytical plate bending solutions stemming from these theories for plates with various boundary conditions are available in the literature. The Navier solution of rectangular simply supported laminated plates can be found in (Srinivas and Rao, 1970; Reddy, 1984; Swaminathan and Ragounadin, 2004). Khdeir and Reddy (1991) conducted the Levy-type solutions of the afore-mentioned theories for antisymmetric cross-ply rectangular laminates. Several other analytical solutions for shear deformable laminated plates can be found in the studies by Khdeir et al. (1987), Oktem and Chaudhuri (2007) and the references therein. Yuemei and Rui (2010) presented an accurate bending analysis of rectangular thin plates with two adjacent edges free and the other clamped or simply supported based on a symplectic geometry approach. An exact solution is formulated in the work by the work by Kobayashi and Turvey (1994) for bending of the annular sector Mindlin plates with two radial edges simply supported and the two circular edges subjected to various boundary conditions.

Exact solution of thick plates, especially based on shear deformations theories, are limited due to their complexities. As a result, researchers have adopted various numerical methods such as finite element method (FEM) (Pandya and Kant, 1988; Dong and Defreitas, 1994; Yildiz and Sarikanat, 2001; Kocak and Hassis, 2003) and the finite strip method (FSM) (Akhras and Li, 2005) for bending analysis of thick plate based on shear deformation plate theories. The use of FEM not only requires appropriate plate elements in order to satisfy continuity and compatibility conditions, but also needs a remeshing procedure for achieving acceptable accuracy. A review of

the recent developments in the finite element analysis of laminated composite plates can be found in the studies by Zhang and Yang (2009).
Some other numerical methods such as differential quadrature method (DQM) and boundary element method (BEM) have also been used to solve thick plate problems. Liew and Han (1997) employed DQM for bending analysis of Reissner-Mindlin plates and further developed it into differential quadrature element method (DQEM) (Liu and Liew, 1998b) to tackle discontinuities in thick plate problems. The differential cubature method (DCM), which is an alternative to the differential equation, was used by Liu and Liew (1998a) for the static analysis of arbitrary shaped plates based on FSDT. The use of an indirect boundary element method (BEM) for Mindlin and Reissner models of thick plates was reported in the studies by De Barcellos and Westphal (1992), and Katsikadelis and Yotis (1993).

Over the past decade, there has been an increasing trend of using meshless methods in which the approximate solution is entirely based on choosing a set of nodes for discretizing the problem domain rather than a mesh. Among these methods are the element free Galerkin method (EFG) (Belytschko et al., 1994) which is an improved form of the diffuse element method (DEM) (Nayroles et al., 1991). EFG has been employed in (Donning and Liu, 1998; Belinha and Dinis, 2006) for analysis of shear deformable plates and laminates. Liu et al. (1995) developed the reproducing kernel particle method (RKPM) in order to enhance the interpolation consistency of the earlier form of the method known as the smoothed particle hydrodynamics (SPH) method. Wang et al. (2002) used RKPM for flexure, vibration and buckling analysis of laminated composite plates based on FSDT. Meshless local Petrov-Galerkin method (MLPG) was formulated by Atluri and Zhu (1998) using a symmetric local weak form that makes it possible to perform integration in a mesh-free sense. The h-p clouds (Duarte and Oden, 1996) is another meshless method that was employed by Garcia et al. (2000) for Mindlin-Reissner thick plates. Wang and Liu (2001) introduced a radial point interpolation method (RPIM) by using radial basis functions (RBFs) for constructing the shape functions. This method was used by Liu et al. (2007) for static, vibration and buckling analysis of shear deformable laminated plates. All these meshfree methods share many common characteristics, while the main differences among them are due to different approaches adopted for constructing the shape functions and obtaining the discrete equations of approximation, in addition to various forms of imposing the essential boundary conditions.

The above mentioned meshless methods use a grid of nodes/points over the computational domain. In the literature, one can find other meshless methods in which a series of points are used over the boundaries. A prerequisite for using such methods is availability of fundamental functions satisfying the governing equations. The method of fundamental solutions (MFS) introduced by Kupradze and Aleksidze (1964) falls in this latter category. In the same category one may find a class of boundary methods known as “Trefftz” methods in which the boundary conditions are satisfied through a variety of weighted residual methods. MFS and BEM are sometimes classified in Trefftz methods. Despite a rich literature for Trefftz method in two/three dimensional heat and solid problems (see Li et al. 2007), and except for studies focusing on construction of Trefftz finite elements (pioneered by Jirousek and co-workers 1977, 1986), few studies can be found addressing the application of the method, in its mesh-less form, to laminated plate bending problems. The reader may refer to the paper by Dong et al. (2004) and

the references therein for further information. Power series are used as the basis functions in this reference.

In this report, a meshless boundary point method introduced by the second author and the co-workers (2009) for the solution of static and time harmonic elasticity problems is extended to solve laminated plate problems. The method uses a series of exponential basis functions (EBFs), satisfying the governing partial differential equations (PDEs), to approximate the solution on the whole domain. The boundary conditions are enforced through a collocation approach on a set of boundary points. In this sense, the method may be classified as Trefftz methods. Comparing with fundamental functions needed in MFS, the EBFs can be easily found for PDEs with constant coefficients. This is the case for variety of plate problems formulated by CLPT, FSDT or TSDT using Cartesian coordinates. As will be discussed later, the in-plane and out-of-plane actions may appear in a coupled formulation depending on the configuration of the layer. Nevertheless this does not create any restrictions for the proposed method in this report since the system of equation is of constant coefficient type. Here we shall show how the appropriate EBFs in each of the aforementioned theories can be found and how one can use them to find semi-analytical solutions for laminated plates with various layer configurations, shapes and boundary conditions.

The layout of the report is as follows. In sections 1 and 2, we shall explore the governing equations and the boundary conditions for CLPT, FSDT and TSDT plate models. Thereafter, in section 3, we shall describe the procedure of evaluating the homogenous and particular solution parts for a generic thick laminated plate. Various numerical examples, for which exact analytical or other numerical solutions are available, shall be presented in section 4 in order to validate the results and demonstrate the accuracy, efficiency and simplicity of the present method. In section 5, we shall summarize the main features of the method.

## 2. GOVERNING EQUATIONS

We consider a plate with uniform total thickness $h$ composed of $N$ orthotropic layers, schematically shown in Figure 1 The midplane is bounded in the domain $\Omega$ in $x_1x_2$-plane with the boundary denoted by $\partial\Omega$. The $m$th layer with the principal material coordinates $(x_1',x_2',x_3')_m$, is oriented at an angle $\theta_m$ to the plate coordinate, $x_1$.

Herein, we deal with the solution of bending problems based on the classical laminated plate theory (CLPT), the first-order shear deformation theory (FSDT), and third-order shear deformation theory (TSDT). The differences among these theories arise from the assumptions and restrictions of displacements through the z thickness direction of the plate.

In this report, indicial notations will be used, in which a repeated or dummy index will be summed over 1 to 2 for Latin lowercase letter, unless otherwise indicated. Consistently, the partial differentiations with respect to $x_i$ coordinates will be represented by the comma-subscript convention.

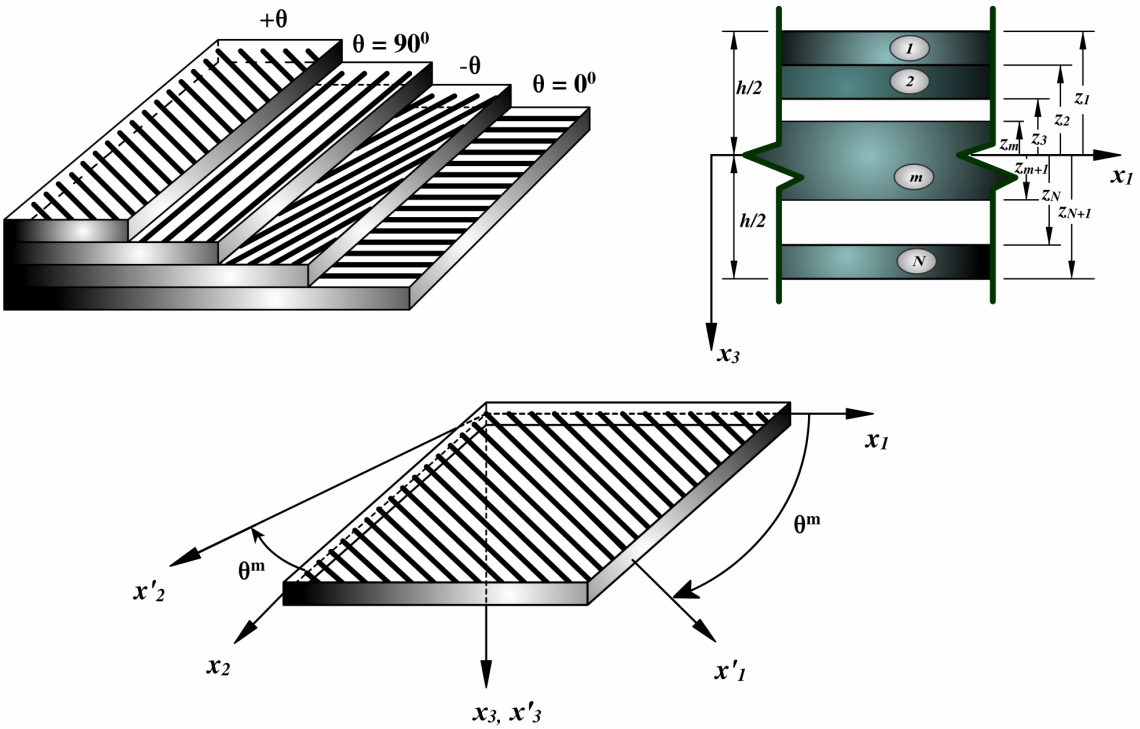


***Figure 1. Plate and lamina coordinate systems and layer numbering in a generic laminated plate.***

In the third-order laminated plate theory proposed by Reddy (2004), assuming cubic expansion of in-plane displacements over the total thickness of the plate leads to the following displacement field

$$\begin{aligned} U_i(x_1,x_2,x_3) &= u_i(x_1,x_2) + x_3\,\phi_i(x_1,x_2) - C_1\,x_3^3\left(\phi_i(x_1,x_2) + u_{3,i}(x_1,x_2)\right) \\ U_3(x_1,x_2,x_3) &= u_3(x_1,x_2) \end{aligned} \tag{1}$$

where $U_i$ $(i=1,2)$ and $U_3$ represent the in-plane and transverse displacement components respectively, $u_i$ $(i=1,2)$ and $u_3$ denote the midplane displacements, and $\phi_i$ $(i=1,2)$ indicates the rotations of the cross sections normal to the in-plane coordinates $x_1$ and $x_2$. Here, $(u_1,\ u_2,\ u_3,\ \phi_1,\ \phi_2)$ are the unknown generalized displacements to be found. Note that one can derive the governing differential equations for the triple theories (i.e. CLPT, FSDT and TSDT) by introducing the following substitutions in (1) (Khdeir et al., 1987)

$$\begin{aligned} &\text{for TSDT:} \quad C_1 = \frac{4}{3h^2} \\ &\text{for FSDT:} \quad C_1 = 0 \\ &\text{for CLPT:} \quad C_1 = 0 \ \text{and} \ \phi_i = -u_{3,i} \end{aligned} \tag{2}$$

The above suggestion holds for the rest of this report unless it is stated otherwise. The strain-displacement relations according to the assumption of small deformations can be written as

$$\varepsilon_{ij} = \varepsilon_{ij}^{(0)} + x_3 \varepsilon_{ij}^{(1)} + x_3^3 \varepsilon_{ij}^{(3)} \tag{3}$$

$$\gamma_{3i} = \gamma_{3i}^{(0)} + x_3^2 \gamma_{3i}^{(2)} \tag{4}$$

where

$$\varepsilon_{ij}^{(0)} = \frac{1}{2}(u_{i,j} + u_{j,i}), \quad \varepsilon_{ij}^{(1)} = \frac{1}{2}(\phi_{i,j} + \phi_{j,i}), \quad \gamma_{3i}^{(0)} = u_{3,i} + \phi_i \tag{5}$$

$$\varepsilon_{ij}^{(3)} = \frac{-C_1}{2}(\phi_{i,j} + \phi_{j,i} + u_{3,ij} + u_{3,ji}), \quad \gamma_{3i}^{(2)} = -C_2\ (u_{3,i} + \phi_i) \tag{6}$$

in which the superscripts 0, 1, 2 and 3 in parentheses represent the constant, linear, square and cubic parts of the strain components' distributions along the plate thickness, respectively. In addition,

$$C_2 = 3\ C_1 \tag{7}$$

where $C_1$ has already been specified for CLPT, FSDT, and TSDT in (2). The stress resultants, per unit length, in terms of the strain components are as follows

$$\begin{aligned}
N_{ij} &= A_{ijkl}\varepsilon_{kl}^{(0)} + B_{ijkl}\varepsilon_{kl}^{(1)} + E_{ijkl}\varepsilon_{kl}^{(3)} \\
M_{ij} &= B_{ijkl}\varepsilon_{kl}^{(0)} + D_{ijkl}\varepsilon_{kl}^{(1)} + F_{ijkl}\varepsilon_{kl}^{(3)} \\
P_{ij} &= E_{ijkl}\varepsilon_{kl}^{(0)} + F_{ijkl}\varepsilon_{kl}^{(1)} + H_{ijkl}\varepsilon_{kl}^{(3)} \\
Q_i &= k_s (A_{3i3j}\gamma_{3j}^{(0)} + D_{3i3j}\gamma_{3j}^{(2)}) \\
R_i &= (D_{3i3j}\gamma_{3j}^{(0)} + F_{3i3j}\gamma_{3j}^{(2)})
\end{aligned} \tag{8}$$

where $N_{ij}$ are the in-plane force resultants, $M_{ij}$ the moment resultants, $Q_i$ the transverse shearing force resultants, and $P_{ij}, R_i$ the higher-order stress resultants, respectively. The parameter $k_s$ in the definition of $Q_i$ denotes the shear correction factor coefficient; which should only be applied in FSDT to correct the discrepancy between the actual transverse shear stresses distributions over the plate thickness and that of evaluated by FSDT (Reddy, 2004). We have taken $k_s = 5/6$ throughout this report.

The overall stiffness of the plate can be expressed in terms of stiffness in each laminate as follows

$$(A_{ijkl},\ B_{ijkl},\ D_{ijkl},\ E_{ijkl},\ F_{ijkl},\ H_{ijkl}) = \sum_{m=1}^{N} \int_{z_m}^{z_{m+1}} \bar{Q}_{ijkl}^{(m)} (1,\ z,\ z^2, z^3,\ z^4,\ z^6)\, dz \tag{9}$$

$$(A_{3i3j},\ D_{3i3j},\ F_{3i3j}) = \sum_{m=1}^{N} \int_{z_m}^{z_{m+1}} \bar{Q}_{3i3j}^{(m)} (1,\ z^2,\ z^4)\, dz \tag{10}$$

where $\bar{Q}_{ijkl}^{(m)}$ and $\bar{Q}_{3i3j}^{(m)}$ denote the in-plane and transverse transformed plane stress stiffness components respectively, and $z_m$, $z_{m+1}$ stand for the lower and upper coordinates of the *m*th lamina, respectively. Although $\bar{\mathbf{Q}}^{(m)}$ is a fourth-order tensor, its components can be distinguished by a double-indicial notation through the following replacements

$$11 \to 1, \quad 22 \to 2, \quad 12 \text{ or } 21 \to 6, \quad 13 \text{ or } 31 \to 5, \quad 23 \text{ or } 32 \to 4 \tag{11}$$

for instance

$$\bar{Q}_{1112}^{(m)} \equiv \bar{Q}_{16}^{(m)}, \ \bar{Q}_{3231}^{(m)} \equiv \bar{Q}_{45}^{(m)}, \ B_{2211} \equiv B_{21}, \ D_{3131} \equiv D_{55}, \ E_{1211} \equiv E_{61}, \ .... \tag{12}$$

The equilibrium equations can be established through the principle of virtual displacement leading to the following relations for TSDT and FSDT with $C1 = 4/3h^2$ and $C1 = 0$, respectively.

$$N_{ij,j} = 0 \tag{13}$$

$$Q_{i,i}^{*} + C_1 P_{ij,ij} + q = 0 \tag{14}$$

$$M_{ij,j}^{*} - Q_i^{*} = 0 \tag{15}$$

and, the equilibrium equations for CLPT are

$$N_{ij,j} = 0 \tag{16}$$

$$M_{ij,ij} + q = 0 \tag{17}$$

where

$$\begin{aligned} M_{ij}^{*} &= M_{ij} - C_1 P_{ij} \\ Q_i^{*} &= Q_i - C_2 R_i \end{aligned} \tag{18}$$

Substitution of (8) into Equations (13)-(18) and together with Equations (3)-(6) results in the governing differential equations in terms of the unknown displacements that can be expressed in a concise matrix form as follows

$$\mathbf{Lu} = \mathbf{q} \tag{19}$$

for FSDT and TSDT $\quad \{\mathbf{u}\} = \{ u_1, u_2, u_3, \phi_1, \phi_2 \}^T, \quad \{\mathbf{q}\} = \{0, 0, q, 0, 0\}^T$

for CLPT $\quad \{\mathbf{u}\} = \{ u_1, u_2, u_3 \}^T, \quad \{\mathbf{q}\} = \{0, 0, q\}^T$

The coefficients of the operator matrix $\mathbf{L}$ for each theory are given in Appendix A.

Generally, the equations governing the bending of laminated plates are a set of coupled partial differential equations with constant coefficients. However, there are some plates with a special sequence of layers such as symmetric ones, in which the stretching-bending coupling stiffness coefficients like $B_{ij}$ and $E_{ij}$ are zero. Therefore, Eqs. (13) and (16) governing the in-plane displacement field are uncoupled from (14), (15) and (17) governing the displacement field due to bending. In this case the in-plane deflections are identically zero in the absence of in-plane edge forces. Therefore, the differential equations reduce to

$$\mathbf{L}^{sub}\mathbf{u} = \mathbf{q} \tag{20}$$

for FSDT and TSDT $\quad \{\mathbf{u}\} = \{u_3,\ \phi_1,\ \phi_2\}^T \quad , \quad \{\mathbf{q}\} = \{q,\ 0,\ 0\}^T$

for CLPT $\quad \{\mathbf{u}\} = \{u_3\}^T \quad , \quad \{\mathbf{q}\} = \{q\}^T$

where $\mathbf{L}^{sub}$ is a sub-matrix consisting of the last three rows and columns of $\mathbf{L}$ in Equation (19) for FSDT and TSDT models, while the only element of $\mathbf{L}^{sub}$ in CLPT models is the last element of $\mathbf{L}$, that is $L_{33}$.

## 3. BOUNDARY CONDITIONS

It should be noted that the general forms of differential equations governing CLPT, FSDT and TSDT models, considering coupling with in-plane actions, are of eighth, tenth and twelfth order, respectively. The order of each theory indicates the number of total boundary conditions on the boundaries of the plate. Half of these boundary conditions are the prescribed ones which must be imposed along the edges of the plate. The prescribed boundary conditions for simply supported (SS), clamped (C), free (F), and sliding (G) edges are described as in Table 1.

The stress resultants in Cartesian coordinate system $(x_1, x_2)$ can be related to those in terms of normal and tangential components with the following transformations

$$\begin{aligned}
&N_{nn} = n_i n_j N_{ij}, \quad M_{nn} = n_i n_j M_{ij}, \quad P_{nn} = n_i n_j P_{ij}, \\
&N_{ns} = n_i s_j N_{ij}, \quad M_{ns} = n_i s_j M_{ij}, \quad P_{ns} = n_i s_j P_{ij}, \\
&Q_n = n_i Q_i, \qquad V_n = Q_n + \frac{\partial M_{ns}}{\partial s} \\
&M^*_{nn} = M_{nn} - C_1 P_{nn} \quad , \quad M^*_{ns} = M_{ns} - C_1 P_{ns} \\
&Q^*_n = Q_n - C_2 R_n, \quad V^*_n = C_1 P_{ij,j} n_i + Q^*_n + C_1 \frac{\partial P_{ns}}{\partial s} \\
&\frac{\partial}{\partial n} = n_i \frac{\partial}{\partial x_i}, \qquad \frac{\partial}{\partial s} = s_i \frac{\partial}{\partial x_i}
\end{aligned} \tag{21}$$

with $\vec{\mathbf{n}} = n_1\vec{i} + n_2\vec{j}$ being the unit outward normal vector, perpendicular to the unit tangential vector $\vec{\mathbf{s}} = s_1\vec{i} + s_2\vec{j}$ such that $\vec{\mathbf{n}} \times \vec{\mathbf{s}} = \vec{k}$, with $\vec{k}$ being the unite vector along $x_3$, at a generic point on the boundary $\partial\Omega$.

**Table 1. The quantities to be defined as boundary conditions in different laminated plate theories. (For the cases tagged by (s. 1) see Remark 1 for the alternatives).**

| Theory | Type | Non-symmetric layers | Symmetric layers |
|---|---|---|---|
| TSDT | SS | $u_s,\ N_{nn},\ u_3,\ P_{nn},\ \phi_s,\ M^*_{nn}$ | $u_3,\ P_{nn},\ \phi_s,\ M^*_{nn}$ |
| | C | $u_s,\ u_n,\ u_3,\ \partial u_3/\partial n,\ \phi_s,\ \phi_n$ | $u_3,\ \partial u_3/\partial n,\ \phi_s,\ \phi_n$ |
| | F | $N_{ns},\ N_{nn},\ V^*_n,\ P_{nn},\ M^*_{ns},\ M^*_{nn}$ (s. 1) | $V^*_n,\ P_{nn},\ M^*_{ns},\ M^*_{nn}$ (s. 1) |
| | G | $N_{ns},\ u_n,\ V^*_n,\ \partial u_3/\partial n,\ M^*_{ns},\ \phi_n$ (s. 1) | $V^*_n,\ \partial u_3/\partial n,\ M^*_{ns},\ \phi_n$ (s. 1) |
| FSDT | SS | $u_s,\ N_{nn},\ u_3,\ \phi_s,\ M_{nn}$ | $u_3,\ \phi_s,\ M_{nn}$ |
| | C | $u_s,\ u_n,\ u_3,\ \phi_s,\ \phi_n$ | $u_3,\ \phi_s,\ \phi_n$ |
| | F | $N_{ns},\ N_{nn},\ Q_n,\ M_{ns},\ M_{nn}$ (s. 1) | $Q_n,\ M_{ns},\ M_{nn}$ (s. 1) |
| | G | $N_{ns},\ u_n,\ Q_n,\ M_{ns},\ \phi_n$ (s. 1) | $Q_n,\ M_{ns},\ \phi_n$ (s. 1) |
| CLPT | SS | $u_s,\ N_{nn},\ u_3,\ M_{nn}$ | $u_3,\ M_{nn}$ |
| | C | $u_s,\ u_n,\ u_3,\ \partial u_3/\partial n$ | $u_3,\ \partial u_3/\partial n$ |
| | F | $N_{ns},\ N_{nn},\ V_n,\ M_{nn}$ | $V_n,\ M_{nn}$ |
| | G | $N_{ns},\ u_n,\ V_n,\ \partial u_3/\partial n$ | $V_n,\ \partial u_3/\partial n$ |

*Remark 1.* In Section 4, it will be demonstrated that thin plate problems can be easily solved by the three theories CLPT, FSDT and TSDT. However, our experience shows that for some special cases the boundary conditions considered for TSDT and FSDT impose extra restriction to the solution when compared with CLPT. This is the case when free and sliding edges are of concern. For instance in plates with symmetric layers, in CLPT just two stress resultants, i.e. $V_n$ and $M_{nn}$, are prescribed while in TSDT and FSDT three conditions, i.e. $Q_n$, $M_{ns}$ and $M_{nn}$, are defined at the edge. This means that when the plate becomes thin, TSDT and FSDT apply stronger condition on $M_{ns}$ while in CLPT its differentiation with respect to $s$ combined with $Q_n$ is restricted to a prescribed value. To unify the conditions for all theories one may define the following stress resultants in TSDT and FSDT for the bending boundary conditions

$$V_n = Q_n + \frac{\partial M_{ns}}{\partial s},\quad \tilde{M}_{ns} = \left(\frac{h}{\tilde{L}}\right)^p M_{ns} \tag{22}$$

In the above relation $h$ denotes the thickness of the plate, $\tilde{L}$ is a characteristic length and $p >> 1$ is an appropriate exponent. The first condition is similar to its counterpart in CLPT while the second one will be active when the thickness is within the order of the characteristic length $h \approx \tilde{L}$. In this report we shall use the mean of the length and width of the rectangular circumscribing the problem domain as $\tilde{L}$ (see Figure 2.a), and $p = 2$. We shall discuss on the effect in Section 4.■

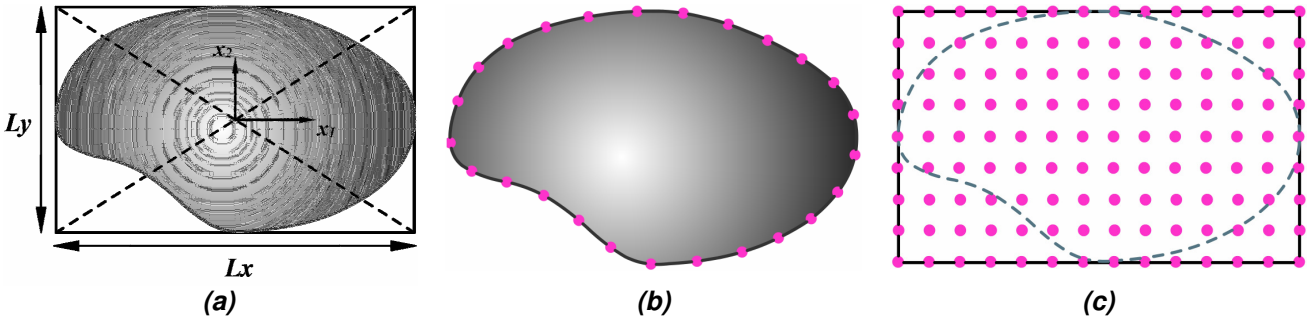


***Figure 2. Plate geometry: (a) The rectangle circumscribing the plate domain and the location of coordinate system; (b) The boundary points; (c) The domain points.***

## 4. SOLUTION PROCEDURE

This section is devoted to develop a solution for the preceding explained boundary value problem in a step-by-step manner. Herein, we use a meshless procedure, firstly proposed by Boroomand et al. (2009) for the solution of static and time harmonic elasticity problems. In this method, the total solutions for the unknown generalized displacements are composed of a homogenous and a particular part. The homogenous solution $\mathbf{u_h}$ and the particular solution $\mathbf{u_p}$ should be determined such that

$$\mathbf{L}\mathbf{u_p} = \mathbf{q} \quad \text{in} \quad \Omega \tag{23}$$

$$\mathbf{L}\mathbf{u_h} = \mathbf{0} \quad \text{in} \quad \Omega \tag{24}$$

$$\mathbf{L_B}(\mathbf{u_h} + \mathbf{u_p}) = \mathbf{L_B}\mathbf{u_h} + \mathbf{L_B}\mathbf{u_p} = \bar{\mathbf{u}}_\mathbf{B} \quad \text{on} \quad \partial\Omega \tag{25}$$

here, $\bar{\mathbf{u}}_\mathbf{B}$ contains the prescribed boundary conditions on $\partial\Omega$. The difference between $\bar{\mathbf{u}}_\mathrm{B}$ and $\mathbf{L}_\mathrm{B}\bar{\mathbf{u}}_\mathrm{p}$ yields a modified form of the boundary conditions, which should be satisfied by the homogenous part of the solution. Therefore, the problem can be redefined as follows

$$\mathbf{L}\mathbf{u_p} = \mathbf{q} \quad \text{in} \quad \Omega \tag{26}$$

$$\mathbf{L}\mathbf{u_h} = \mathbf{0} \quad \text{in} \quad \Omega \tag{27}$$

$$\mathbf{L_B}\mathbf{u_h} = \bar{\mathbf{u}}_\mathbf{h} \quad \text{on} \quad \partial\Omega \quad \text{where} \quad \bar{\mathbf{u}}_\mathbf{h} = \bar{\mathbf{u}}_\mathbf{B} - \mathbf{L_B}\mathbf{u_p} \tag{28}$$

In the following subsections, firstly, we shall explain a method based on the summation of a series of exponential basis functions (EBFs) with unknown coefficients for handling the

prescribed boundary conditions. In this regard, we shall employ two forms of strategies for selecting the EBFs, one based on the projection of the boundary measures on the boundary values of the basis, and another based on the numerical experiments. Secondly, the loading conditions will be dealt with through a numeric procedure similar to that used in the homogenous solution.

### 4.1 Homogenous solution

Solution of the homogenous part of the response involves solving the problem defined in (27) and (28). For convenience, we temporarily set aside indicial notation and rename the axes and the displacement components as

$$x = x_1, \quad y = x_2, \quad z = x_3, \quad u = u_1, \quad v = u_2, \quad w = u_3 \tag{29}$$

Now we assume $\mathbf{u_h}$ in terms of the EBFs as

$$\mathbf{u_h}(x, y, \alpha, \beta) = \mathbf{h}_{(\alpha,\beta)} e^{\alpha x + \beta y} \qquad \forall (\mathrm{x}, \mathrm{y}) \in \Omega \quad \text{and} \quad (\alpha, \beta) \in \mathbb{C}^2 \tag{30}$$

where $\mathbf{h}_{(\alpha,\beta)}$ is a vector containing the contribution of the basis function to the generalized displacement coefficients, that is

for FSDT and TSDT

$$\begin{cases} \mathbf{h}_{(\alpha,\beta)} = \left\{ h^u,\ h^v,\ h^w,\ h^{\phi_x},\ h^{\phi_y} \right\}^T & \text{for non-symmetric laminae} \\ \mathbf{h}_{(\alpha,\beta)} = \left\{ h^w,\ h^{\phi_x},\ h^{\phi_y} \right\}^T & \text{for symmetric laminae} \end{cases} \tag{31}$$

for CLPT

$$\begin{cases} \mathbf{h}_{(\alpha,\beta)} = \left\{ h^u,\ h^v,\ h^w \right\}^T & \text{for non-symmetric laminae} \\ \mathbf{h}_{(\alpha,\beta)} = \left\{ h^w \right\} & \text{for symmetric laminae} \end{cases} \tag{32}$$

Substitution of (30) in (27) results in the following matrix relation

$$\mathbf{L}_{(\alpha,\beta)} \mathbf{h}_{(\alpha,\beta)} = \mathbf{0} \tag{33}$$

where the constant coefficients of the matrix $\mathbf{L}_{(\alpha,\beta)}$ can be obtained from the elements of $\mathbf{L}$ in (19), listed in Appendix A, with the following replacements

$$d_1^m \equiv \alpha^m, \qquad d_2^m \equiv \beta^m \tag{34}$$

In the above relations, the superscript $m$ in $d_1^m$ and $d_2^m$ denotes the order of differentiation with respect to $x$ and $y$ coordinates respectively, while at the same time it indicates the $m$th power of $\alpha$ and $\beta$ when the EBFs are used as the solution.

For having non-trivial solution for the unknowns, the determinant of the coefficient matrix $\mathbf{L}_{(\alpha,\beta)}$ in (33) must be set to zero. The resulted characteristic equation can be written in a symbolic form as

$$Det\ [\mathbf{L}_{(\alpha,\beta)}]=0 \quad \Rightarrow \quad \Psi(\alpha,\ \beta)=0 \tag{35}$$

Herein, $\Psi(\alpha,\ \beta)=0$ is an algebraic (polynomial) equation, from which one may find $\alpha$ in terms of $\beta$ or vice versa. The characteristic vector $\mathbf{h}_{(\alpha,\ \beta)}$ is the nontrivial solution of the homogenous system of linear equations, defined in (33), which is equivalent to the null-space vector of matrix $\mathbf{L}_{(\alpha,\beta)}$. It should be noted that the total solution in (27) contains all the EBFs obtained from both cases, that is when $\alpha$ is written in terms of $\beta$ and vice versa as

$$\alpha_l = f_l(\beta) \qquad l=1,.....,r \tag{36}$$

or

$$\beta_l = g_l(\alpha) \qquad l=1,.....,r \tag{37}$$

This may be performed either explicitly by finding the functions or numerically by choosing one and calculating the roots of the algebraic equation (35). It must also be noted that $\alpha$ and $\beta$ in (36) and (37) may take on complex values. Therefore, the solution to (27) may be written as

$$\mathbf{u}_\mathbf{h} = \int_{\Omega_\beta} \left\{ \sum_{l=1}^{r} C^{\,l}_{(f_l(\beta),\ \beta)} \mathbf{h}^l_{(f_l(\beta),\ \beta)} e^{f_l(\beta)x+\beta y} \right\} d\,\Omega_\beta + \int_{\Omega_\alpha} \sum_{l=1}^{r} C^{\,l}_{(\alpha,\ g_l(\alpha))} \mathbf{h}^l_{(\alpha,\ g_l(\alpha))} e^{\alpha x+g_l(\alpha)y}\, d\,\Omega_\alpha \tag{38}$$

where $\Omega_\beta$ and $\Omega_\alpha$ are two appropriate areas or loci in the Gaussian plane and $r$ is the number of roots derived from the characteristic equation. In general laminates, we may have eight, ten and twelve distinct roots with four, five and six pairs of complex conjugates for CLPT, FSDT and TSDT plate theories, respectively. The unknown coefficients $C^l_{(f_l(\beta),\ \beta)}$ and $C^l_{(\alpha,\ g_l(\alpha))}$ in (38) are to be found so that the boundary conditions in (28) are satisfied. This, if not possible, is a very difficult task for most problems. However, one may think of a discrete form of (38), for instance when the integral is to be calculated numerically, and simply write

$$\mathbf{u}_\mathbf{h} = \sum_j \left\{ \sum_{l=1}^{r} c_j^l \mathbf{h}^l_{(f_l(\beta_j),\ \beta_j)} e^{f_l(\beta_j)x+\beta_j y} + \sum_{l=1}^{r} \bar{c}_j^l \mathbf{h}^l_{(\alpha_j,\ g_l(\alpha_j))} e^{\alpha_j x+g_l(\alpha_j)y} \right\} \tag{39}$$

with $c_j^l$ and $\bar{c}_j^l$ being new coefficients when $\beta_j$ and $\alpha_j$ are chosen. For convenience, we summarize the above expression as follows

$$\mathbf{u_h} = \sum_i c_i \mathbf{h}_{(\alpha_i,\beta_i)}\ e^{\alpha_i x+\beta_i y} \tag{40}$$

Note that, in (39) and (40), the subscript $i$ (or $j$) is an index for counting the number of EBFs, which should not be confused with the one used in the indicial convention for describing the governing equations.

It should be noted that it is neither feasible nor necessary to express the EBFs and their corresponding characteristic vectors in (40), explicitly, in terms of the known quantities. This is a result of the dependence of polynomial coefficients on the lamination schemes and stiffness coefficients that make it almost impossible to write its roots for a generic laminate, symbolically.

The above-mentioned procedure is straightforward as long as the roots of the characteristic equation (35) are distinct, which is true in many laminated plates except for single layer isotropic ones. In this case, the characteristic equation might yield multiple roots. To illustrate how to handle this case of degeneracy, let us consider a homogenous isotropic plate of thickness $h$ with Young's modulus $E$ and Poisson's ratio $\nu$. Since the in-plane and bending deformations in single layer plates are uncoupled, we may use the form of the differential equations introduced in (20). The procedure of determining the EBFs for CLPT, FSDT and TSDT are described as follows.

*a) For CLPT*

Substitution of the $i$th EBF from (40) (i.e. $h_i^w e^{\alpha_i x+\beta_i y}$) into the homogenous form of (20) yields the following homogenous equation and characteristic equation for an isotropic single layer plate based on CLPT

$$\mathbf{L}^{sub}_{(\alpha_i,\,\beta_i)}\mathbf{h}_{(\alpha_i,\,\beta_i)} = \mathbf{0} \quad \text{with} \quad \mathbf{h}_{(\alpha_i,\,\beta_i)} = \left\{h_i^w\right\}^T \tag{41}$$

which gives

$$\frac{Eh^3}{12(1-\nu^2)}(\alpha_i^4 + 2\alpha_i^2\beta_i^2 + \beta_i^4)h_i^w = 0 \tag{42}$$

or

$$\Psi(\alpha_i\,,\,\beta_i) = (\alpha_i^2 + \beta_i^2)^2 = 0 \tag{43}$$

If $\beta_i$ is evaluated in terms of $\alpha_i$ we have

$$\beta_i = -\mathbf{i}\alpha_i \quad \text{(double roots)}, \qquad h_i^w = 1 \tag{44}$$

$$\beta_i = \mathbf{i}\alpha_i \quad \text{(double roots)}, \qquad h_i^w = 1 \tag{45}$$

in the above relations $\mathbf{i}=\sqrt{-1}$.

Note that $h_i^w$ can be any arbitrary value. Here, we have adopted $h_i^w=1$ for convenience. From Eqs. (44) and (45), we obtain only two independent EBFs, while the other two can be determined by assuming the EBFs in the following form

$$\mathrm{u}_{\mathrm{h}}^{i}=(f_i^w x+g_i^w y+d_i^w)e^{\alpha_i x+\beta_i y} \tag{46}$$

The above relation for the EBFs deduce the following characteristic equation

$$(\alpha_i^2+\beta_i^2)((\alpha_i^2 x+\beta_i^2 x+4\alpha_i)f_i^w+(\alpha_i^2 y+\beta_i^2 y+4\beta_i)g_i^w+(\alpha_i^2+\beta_i^2)d_i^w)=0 \tag{47}$$

which is identically zero for $\beta_i=-\mathbf{i}\alpha_i$ and $\beta_i=\mathbf{i}\alpha_i$. For having non-trivial and distinct EBFs from those obtained in (44) and (45), $f_i^w$ and $g_i^w$ should not be zero simultaneously. Any other arbitrary values can be adopted for $f_i^w$, $g_i^w$ and $d_i^w$; here, we take $f_i^w=g_i^w=1$ and $d_i^w=0$. Therefore, we obtain four distinct EBFs, when $\beta_i$ is written in terms of $\alpha_i$. The homogenous solution for this case can be written as

$$\mathrm{u}_{\mathrm{h}}=\sum_i\left(c_i^1 e^{\alpha_i(x+\mathbf{i}y)}+c_i^2 e^{\alpha_i(x-\mathbf{i}y)}+c_i^3(x+y)e^{\alpha_i(x+\mathbf{i}y)}+c_i^4(x+y)e^{\alpha_i(x-\mathbf{i}y)}\right) \tag{48}$$

The solution for the other case (i.e. when $\beta_i$ is written in terms of $\alpha_i$) is determined analogously and added to the above solution.

*Remark 2.* The reader may note that there is a possibility of obtaining more repeating roots for $\beta_i$ (or $\alpha_i$) when $\alpha_i$ is chosen as zero which gives four roots as $\beta_i=0$. With the same logic used in writing (46), one can easily show that the basis functions are in fact the monomials of a third order complete polynomial. Our numerical experience shows that adding such bases to the solution does not affect the final results. ■

*b) For FSDT*

The homogenous system of equations and the characteristic equation for an isotropic single layer plate based on FSDT are

$$\mathbf{L}^{sub}_{(\alpha_i,\,\beta_i)}\mathbf{h}_{(\alpha_i,\,\beta_i)}=\mathbf{0} \quad \text{with} \quad \mathbf{h}_{(\alpha_i,\,\beta_i)}=\left\{h_i^w,\ h_i^{\phi_x},\ h_i^{\phi_y}\right\}^T \tag{49}$$

$$\Psi(\alpha_i,\,\beta_i)=(\alpha_i^2+\beta_i^2)^2(h^2(\alpha_i^2+\beta_i^2)-12k_s)=0 \tag{50}$$

where the constant coefficients of $\mathbf{L}^{sub}_{(\alpha_i,\,\beta_i)}$ matrix may be obtained from those of $\mathbf{L}^{sub}$ in (20) with similar replacements described in (34). By evaluating $\beta_i$ in terms of $\alpha_i$ from the characteristic equation, we have

$$\beta_i = -\mathbf{i}\alpha_i \quad \text{(double roots)}, \qquad \mathbf{h}_{(\alpha_i,\beta_i)} = \{-\mathbf{i},\ \mathbf{i}\alpha_i,\ \alpha_i\}^T \tag{51}$$

$$\beta_i = \mathbf{i}\alpha_i \quad \text{(double roots)}, \qquad \mathbf{h}_{(\alpha_i,\beta_i)} = \{\mathbf{i},\ -\mathbf{i}\alpha_i,\ \alpha_i\}^T \tag{52}$$

$$\beta_i = -\frac{\sqrt{-h^2\alpha_i^2 + 12k_s}}{h} \quad \text{(single root)}, \qquad \mathbf{h}_{(\alpha_i,\beta_i)} = \left\{0,\ \sqrt{-h^2\alpha_i^2 + 12k_s},\ h\alpha_i\right\}^T \tag{53}$$

$$\beta_i = \frac{\sqrt{-h^2\alpha_i^2 + 12k_s}}{h} \quad \text{(single root)}, \qquad \mathbf{h}_{(\alpha_i,\beta_i)} = \left\{0,\ -\sqrt{-h^2\alpha_i^2 + 12k_s},\ h\alpha_i\right\}^T \tag{54}$$

It is obvious that from the above derivations only four EBFs can be obtained since there is only one independent null-space associated with each of the double roots in Equations (51) and (52). The missing EBFs can be found by considering a modified form of them as follows

$$\mathbf{u}_{\mathbf{h}}^{i} = \left[\begin{Bmatrix} f_i^{w} \\ f_i^{\phi_x} \\ f_i^{\phi_y} \end{Bmatrix} x + \begin{Bmatrix} g_i^{w} \\ g_i^{\phi_x} \\ g_i^{\phi_y} \end{Bmatrix} y + \begin{Bmatrix} d_i^{w} \\ d_i^{\phi_x} \\ d_i^{\phi_y} \end{Bmatrix}\right] e^{\alpha_i x + \beta_i y} \tag{55}$$

Substituting the above equation into the homogenous form of (20), and also by rearranging it, the following system of equations are obtained

$$\left\{\mathbf{A}_{(\alpha_i,\beta_i)}\left[\mathbf{f}_{(\alpha_i,\beta_i)}x + \mathbf{g}_{(\alpha_i,\beta_i)}y\right] + \left[\mathbf{B}_{(\alpha_i,\beta_i)}\mathbf{f}_{(\alpha_i,\beta_i)} + \mathbf{C}_{(\alpha_i,\beta_i)}\mathbf{g}_{(\alpha_i,\beta_i)} + \mathbf{A}_{(\alpha_i,\beta_i)}\mathbf{d}_{(\alpha_i,\beta_i)}\right]\right\} e^{\alpha_i x + \beta_i y} = \mathbf{0} \tag{56}$$

with the coefficient matrices $\mathbf{A}_{(\alpha_i,\beta_i)}$, $\mathbf{B}_{(\alpha_i,\beta_i)}$ and $\mathbf{C}_{(\alpha_i,\beta_i)}$ given by

$$\mathbf{A}_{(\alpha_i,\beta_i)} = \begin{bmatrix} -\frac{Ehk_s(\alpha_i^2+\beta_i^2)}{2(1+\nu)} & -\frac{Ehk_s\alpha_i}{2(1+\nu)} & -\frac{Ehk_s\beta_i}{2(1+\nu)} \\ -\frac{Ehk_s\alpha_i}{2(1+\nu)} & \frac{Eh(h^2(2\alpha_i^2+\beta_i^2(1-\nu))-12k_s(1-\nu))}{24(1-\nu^2)} & \frac{Eh^3k_s\alpha_i\beta_i}{24(1-\nu)} \\ -\frac{Ehk_s\beta_i}{2(1+\nu)} & \frac{Eh^3k_s\alpha_i\beta_i}{24(1-\nu)} & \frac{Eh(h^2(2\beta_i^2+\alpha_i^2(1-\nu))-12k_s(1-\nu))}{24(1-\nu^2)} \end{bmatrix},$$

$$\mathbf{B}_{(\alpha_i,\beta_i)} = \begin{bmatrix} -\frac{Ehk_s\alpha_i}{(1+\nu)} & -\frac{Ehk_s}{2(1+\nu)} & 0 \\ -\frac{Ehk_s}{2(1+\nu)} & \frac{Eh^3\alpha_i}{6(1-\nu^2)} & \frac{Eh^3\beta_i}{24(1-\nu)} \\ 0 & \frac{Eh^3\beta_i}{24(1-\nu)} & \frac{Eh^3\alpha_i}{12(1+\nu)} \end{bmatrix}, \quad \mathbf{C}_{(\alpha_i,\beta_i)} = \begin{bmatrix} -\frac{Ehk_s\beta_i}{(1+\nu)} & 0 & -\frac{Ehk_s}{2(1+\nu)} \\ 0 & \frac{Eh^3\beta_i}{12(1+\nu)} & \frac{Eh^3\alpha_i}{24(1-\nu)} \\ -\frac{Ehk_s}{2(1+\nu)} & \frac{Eh^3\alpha_i}{24(1-\nu)} & \frac{Eh^3\beta_i}{6(1-\nu^2)} \end{bmatrix} \tag{57}$$

Considering the fact that the matrix $\mathbf{A}_{(\alpha_i,\beta_i)}$ in (57) is the same as $\mathbf{L}^{sub}_{(\alpha_i,\beta_i)}$ in (49), and its determinant is zero for the double roots, we may write

$$\begin{aligned}
&\beta_i=-\mathbf{i}\alpha_i \;\Rightarrow\; \mathbf{f}_{(\alpha_i,\beta_i)}=a\{-\mathbf{i},\ \mathbf{i}\alpha_i,\ \alpha_i\}^{\mathrm{T}}\ ,\quad \mathbf{g}_{(\alpha_i,\beta_i)}=b\{-\mathbf{i},\ \mathbf{i}\alpha_i,\ \alpha_i\}^{\mathrm{T}}\\
&\beta_i=\mathbf{i}\alpha_i \;\Rightarrow\; \mathbf{f}_{(\alpha_i,\beta_i)}=a\{\mathbf{i},\ -\mathbf{i}\alpha_i,\ \alpha_i\}^{\mathrm{T}},\quad \mathbf{g}_{(\alpha_i,\beta_i)}=b\{\mathbf{i},\ -\mathbf{i}\alpha_i,\ \alpha_i\}^{\mathrm{T}}
\end{aligned}\tag{58}$$

Setting to zero the last term on the left hand side of (56) yields

$$\begin{aligned}
&\beta_i=-\mathbf{i}\alpha_i \;\Rightarrow\; \mathbf{A}_{(\alpha_i,\beta_i)}\mathbf{d}_{(\alpha_i,\beta_i)}=-(a\mathbf{B}_{(\alpha_i,\beta_i)}+b\mathbf{C}_{(\alpha_i,\beta_i)})\{-\mathbf{i},\ \mathbf{i}\alpha_i,\ \alpha_i\}^{\mathrm{T}}\\
&\beta_i=\mathbf{i}\alpha_i \;\Rightarrow\; \mathbf{A}\mathbf{d}_{(\alpha_i,\beta_i)}=-(a\mathbf{B}_{(\alpha_i,\beta_i)}+b\mathbf{C}_{(\alpha_i,\beta_i)})\{\mathbf{i},\ -\mathbf{i}\alpha_i,\ \alpha_i\}^{\mathrm{T}}
\end{aligned}\tag{59}$$

Upon considering $a$ and $b$ as a set of new unknown coefficients, any of the above relations will be a set of just two independent equations with three unknowns $(d_i^w,\ d_i^{\phi_x},\ d_i^{\phi_y})$, which can be solved by choosing one ($d_i^w$ for instance) and finding the other two. Therefore,

$$\begin{aligned}
&\beta_i=-\mathbf{i}\alpha_i \;\Rightarrow\; \mathbf{d}_{(\alpha_i,\beta_i)}=a\begin{Bmatrix}0.5\alpha_i\\ -\mathbf{i}h^2{\alpha_i}^2\lambda-0.5(\alpha_i^2-2\mathbf{i})\\ -h^2{\alpha_i}^2\lambda+0.5{\alpha_i}^2\mathbf{i}\end{Bmatrix}+b\begin{Bmatrix}0.5\alpha_i\\ -h^2{\alpha_i}^2\lambda-0.5{\alpha_i}^2\\ h^2\alpha_i^2\lambda\mathbf{i}+0.5\mathbf{i}(\alpha_i^2+2)\end{Bmatrix}\\
&\beta_i=\mathbf{i}\alpha_i \;\Rightarrow\; \mathbf{d}_{(\alpha_i,\beta_i)}=a\begin{Bmatrix}0.5\alpha_i\\ h^2\alpha_i^2\lambda\mathbf{i}-0.5(\alpha_i^2+2\mathbf{i})\\ -h^2\alpha_i^2\lambda-0.5\mathbf{i}\alpha_i^2\end{Bmatrix}+b\begin{Bmatrix}0.5\alpha_i\\ -h^2\alpha_i^2\lambda-0.5\alpha_i^2\\ -h^2\alpha_i^2\lambda\mathbf{i}-0.5\mathbf{i}(\alpha_i^2+2)\end{Bmatrix}
\end{aligned}\tag{60}$$

in which $\lambda=1/(3k_s(\nu-1))$.

Our experience shows that excellent solution may be obtained by reducing the number of basis and assuming $a=b=1$. This leads to the following forms

$$\begin{aligned}
&\beta_i=-\mathbf{i}\alpha_i \;\Rightarrow\; \mathbf{d}_{(\alpha_i,\beta_i)}=\begin{Bmatrix}\alpha_i\\ -h^2{\alpha_i}^2\lambda(1+\mathbf{i})-(\alpha_i^2-\mathbf{i})\\ h^2\alpha_i^2\lambda(\mathbf{i}-1)+\mathbf{i}(\alpha_i^2+1)\end{Bmatrix}\\
&\beta_i=\mathbf{i}\alpha_i \;\Rightarrow\; \mathbf{d}_{(\alpha_i,\beta_i)}=\begin{Bmatrix}\alpha_i\\ h^2{\alpha_i}^2\lambda(\mathbf{i}-1)-(\alpha_i^2+\mathbf{i})\\ -h^2\alpha_i^2(\mathbf{i}+1)-\mathbf{i}(\alpha_i^2+1)\end{Bmatrix}
\end{aligned}\tag{61}$$

Hence, the missing EBFs can be written as

$$\beta_i = -\mathbf{i}\alpha_i \;\Rightarrow\; \mathbf{h}_{(\alpha_i,\beta_i)} = \begin{Bmatrix} -\mathbf{i} \\ \mathbf{i}\alpha_i \\ \alpha_i \end{Bmatrix} x + \begin{Bmatrix} -\mathbf{i} \\ \mathbf{i}\alpha_i \\ \alpha_i \end{Bmatrix} y + \begin{Bmatrix} \alpha_i \\ -h^2{\alpha_i}^2\lambda(1+\mathbf{i}) - (\alpha_i^2 - \mathbf{i}) \\ h^2\alpha_i^2\lambda(\mathbf{i}-1) + \mathbf{i}(\alpha_i^2+1) \end{Bmatrix} \tag{62}$$

$$\beta_i = \mathbf{i}\alpha_i \;\Rightarrow\; \mathbf{h}_{(\alpha_i,\beta_i)} = \begin{Bmatrix} \mathbf{i} \\ -\mathbf{i}\alpha_i \\ \alpha_i \end{Bmatrix} x + \begin{Bmatrix} \mathbf{i} \\ -\mathbf{i}\alpha_i \\ \alpha_i \end{Bmatrix} y + \begin{Bmatrix} \alpha_i \\ h^2{\alpha_i}^2\lambda(\mathbf{i}-1) - (\alpha_i^2 + \mathbf{i}) \\ -h^2\alpha_i^2\lambda(\mathbf{i}+1) - \mathbf{i}(\alpha_i^2+1) \end{Bmatrix} \tag{63}$$

So far, we have six independent EBFs, defined in (51)-(54) and (62)-(63) for the case that $\beta_i$ is written in terms of $\alpha_i$. The procedure for the other case, that is when $\alpha_i$ is calculated in terms of $\beta_i$ is the same.

*Remark 3*. It may be noted that if $\alpha_i$ is chosen so that $12k_s - h^2\alpha_i^2 = 0$ in (53) and (54), then a pair of roots as $\beta_i = 0$ is obtained and thus some EBFs will be missed again. The procedure of finding the new EFBs is similar to that described above. Moreover, similar to CLPT, one may obtain more repeating roots for $\beta_i$ (or $\alpha_i$) when $\alpha_i$ is chosen as zero in (51) and (52) which gives four roots as $\beta_i = 0$. With the same logic used in writing (55), we may use a third order complete polynomial with unknown vector coefficients to find the bases. As mentioned earlier, our numerical experience in this case also shows that adding such bases to the solution does not affect the final results. ■

*c) For TSDT*

The characteristic equation for an isotropic single layer plate based on TSDT with $C_1 = 4/3h^2$ and $C_2 = 3C_1$ is

$$\Psi(\alpha_i,\, \beta_i) = (\alpha_i^2 + \beta_i^2)^2(17h^2(\alpha_i^2 + \beta_i^2) - 168)(h^2(\alpha_i^2 + \beta_i^2) + 420(\nu - 1)) = 0 \tag{64}$$

when $\beta_i$ is evaluated in terms of $\alpha_i$ from the characteristic equation, we have

$$\beta_i = -\mathbf{i}\alpha_i \quad \text{(double roots)}, \qquad \mathbf{h}_{(\alpha_i,\beta_i)} = \{-\mathbf{i},\ \mathbf{i}\alpha_i,\ \alpha_i\}^T \tag{65}$$

$$\beta_i = \mathbf{i}\alpha_i \quad \text{(double roots)}, \qquad \mathbf{h}_{(\alpha_i,\beta_i)} = \{\mathbf{i}, -\mathbf{i}\alpha_i,\ \alpha_i\}^T \tag{66}$$

$$\beta_i = -\frac{\sqrt{168 - 17h^2\alpha_i^2}}{\sqrt{17}h} \quad \text{(single root)}, \qquad \mathbf{h}_{(\alpha_i,\beta_i)} = \left\{0,\ \sqrt{168 - 17h^2\alpha_i^2},\ \sqrt{17}h\alpha_i\right\}^T \tag{67}$$

$$\beta_i = \frac{\sqrt{168 - 17h^2\alpha_i^2}}{\sqrt{17}h} \quad \text{(single root)}, \qquad \mathbf{h}_{(\alpha_i,\beta_i)} = \left\{0, -\sqrt{168 - 17h^2\alpha_i^2},\ \sqrt{17}h\alpha_i\right\}^T \tag{68}$$

$$\beta_i = -\frac{\sqrt{420(1-\nu)-h^2\alpha_i^2}}{h} \quad \text{(single root)}, \quad \mathbf{h}_{(\alpha_i,\beta_i)} = \left\{-4h,\ -h\alpha_i,\ \sqrt{420(1-\nu)-h^2\alpha_i^2}\right\}^T \tag{69}$$

$$\beta_i = \frac{\sqrt{420(1-\nu)-h^2\alpha_i^2}}{h} \quad \text{(single root)}, \quad \mathbf{h}_{(\alpha_i,\beta_i)} = \left\{4h,\ h\alpha_i,\ \sqrt{420(1-\nu)-h^2\alpha_i^2}\right\}^T \tag{70}$$

The above equations yield six distinct EBFs, while the missed EBFs corresponding to the double roots can be found by considering a modified form of them similar to (55). Conducting similar procedure to that described for FSDT, we first obtain two sets of relations as (60) with $\lambda$ replaced by $\eta$ and then we choose $a=b=1$ to get

$$\beta_i = -\mathbf{i}\alpha_i \ \Rightarrow\ \mathbf{h}_{(\alpha_i,\beta_i)} = \begin{Bmatrix} -\mathbf{i} \\ \mathbf{i}\alpha_i \\ \alpha_i \end{Bmatrix} x + \begin{Bmatrix} -\mathbf{i} \\ \mathbf{i}\alpha_i \\ \alpha_i \end{Bmatrix} y + \begin{Bmatrix} \alpha_i \\ -h^2{\alpha_i}^2\eta(1+\mathbf{i})-(\alpha_i^2-\mathbf{i}) \\ h^2\alpha_i^2\eta(\mathbf{i}-1)+\mathbf{i}(\alpha_i^2+1) \end{Bmatrix} \tag{71}$$

$$\beta_i = \mathbf{i}\alpha_i \ \Rightarrow\ \mathbf{h}_{(\alpha_i,\beta_i)} = \begin{Bmatrix} \mathbf{i} \\ -\mathbf{i}\alpha_i \\ \alpha_i \end{Bmatrix} x + \begin{Bmatrix} \mathbf{i} \\ -\mathbf{i}\alpha_i \\ \alpha_i \end{Bmatrix} y + \begin{Bmatrix} \alpha_i \\ h^2{\alpha_i}^2\eta(\mathbf{i}-1)-(\alpha_i^2+\mathbf{i}) \\ -h^2\alpha_i^2\eta(\mathbf{i}+1)-\mathbf{i}(\alpha_i^2+1) \end{Bmatrix} \tag{72}$$

where $\eta = 1/(2(\nu-1))$.

Now, we have eight independent EBFs, defined in (65)-(72) for the case that $\beta_i$ is written in terms of $\alpha_i$. The procedure for the other case, that is when $\alpha_i$ is calculated in terms of $\beta_i$ is the same.

*Remark 4.* As mentioned in Remark 3 for FSDT, there are some cases for which one may obtain more repeating roots. In view of (67) and (68), if $\alpha_i$ is chosen so that $168-17h^2\alpha_i^2=0$ then a pair of roots as $\beta_i=0$ is obtained. Also, referring to (69) and (70), in case that $\alpha_i$ is chosen so that $420(1-\nu)-h^2\alpha_i^2=0$, another pair of roots as $\beta_i=0$ is obtained and thus some EBFs will be missed again. For $\alpha_i=0$ we find four roots as $\beta_i=0$. The procedure of finding the new EFBs for the former two cases is similar to that described above but for the latter case we should consider a third order complete polynomial with unknown vector coefficients to find the bases (see also Remark 3). ■

### 4.2 Imposition of the boundary conditions

In the present work, the boundary conditions will be satisfied through a collocation approach over a set of discrete points on the boundary $\partial\Omega$. The number of boundary points M is not necessarily equal to or more than the number of EBFs (i.e. N) used for approximating the solution over the domain. Thus, with the use of (40) we may write

$$\bar{\mathbf{U}} = \sum_{i=1}^{N} C_i \mathbf{V}_i \tag{73}$$

where $C_i$ is a constant coefficient proportional to $c_i$ in (40), and $\bar{\mathbf{U}}$ and $\mathbf{V}_i$ are vectors that, respectively, contain the modified prescribed boundary conditions at each boundary point and the contribution of *i*th EBF to the same boundary points, that is

$$\bar{\mathbf{U}} = \left\{ (\bar{\mathbf{u}}_{\mathrm{h}})_1 \quad (\bar{\mathbf{u}}_{\mathrm{h}})_2 \quad .... \quad (\bar{\mathbf{u}}_{\mathrm{h}})_j \quad .... \quad (\bar{\mathbf{u}}_{\mathrm{h}})_M \right\}^T \tag{74}$$

$$\mathbf{V}_i = \frac{1}{s_i} \left\{ (\bar{\mathbf{v}}_i)_1 \quad (\bar{\mathbf{v}}_i)_2 \quad .... \quad (\bar{\mathbf{v}}_i)_j \quad .... \quad (\bar{\mathbf{v}}_i)_M \right\}^T \tag{75}$$

where $(\bar{\mathbf{u}}_{\mathrm{h}})_j$ is the difference between the prescribed boundary condition and that of the particular solution at the *j*th boundary point, and $(\bar{\mathbf{v}}_i)_j$ is the contribution of the *i*th basis function to the prescribed value at the same point. Considering the *i*th basis function (i.e. $\mathbf{h}_{(\alpha_i,\beta_i)} e^{\alpha_i x + \beta_i y}$) and the prescribed boundary condition at the *j*th boundary point, one may write

$$(\bar{\mathbf{u}}_{\mathrm{h}})_j = (\bar{\mathbf{u}}_{\mathrm{B}})\big|_{x=x_j, y=y_j} + (\mathbf{B}\mathbf{u}_{\mathrm{P}})\big|_{x=x_j, y=y_j}, \qquad \forall (x_j, y_j) \in \partial\Omega, \ j = 1, \ ..., \ M \tag{76}$$

$$(\bar{\mathbf{v}}_i)_j = (\mathbf{B}(\mathbf{h}_{(\alpha_i,\beta_i)} e^{\alpha_i x + \beta_i y}))\Big|_{x=x_j, y=y_j}, \qquad \forall (x_j, y_j) \in \partial\Omega, \ j = 1, \ ..., \ M \tag{77}$$

where M is the total number of boundary points (see Figure 2.b.), and $\mathbf{B}$ is the boundary operator matrix, whose components for different boundary types for TSDT, FSDT and CLPT are given in Appendix B. In Equation (75), the parameter $s_i$ plays the role of a scaling factor for normalizing $\mathbf{V}_i$. Here, the scaling factor is chosen as the maximum element of $\mathbf{V}_i$ in terms of its absolute value, that is

$$s_i = (V_i)_\zeta \quad \text{where} \quad (V_i)_\zeta = \max_{1 \le j \le M} \left( \left| (V_i)_j \right| \right) \tag{78}$$

in which $(V_i)_\zeta$ is an element of $\mathbf{V}_i$ whose absolute value is maximum. Other norms such as the Hermitian length of $\mathbf{V}_i$ may also be used. Thus, the coefficient $c_i$ in (40) can be related to $C_i$ introduced in (73) as follows

$$c_i = \frac{1}{s_i} C_i \tag{79}$$

The only unknown to be found in the above procedure is the constant coefficients $C_i$. This can be done by the transformation used in (Boroomand and Mossaiby, 2005a, b, 2006) and explained in (Boroomand et al., 2009), in which $C_i$ is written as

$$C_i = \mathbf{V}_i^{\mathrm{T}} \mathbf{R}_{\mathrm{h}} \bar{\mathbf{U}}, \qquad \mathbf{R}_{\mathrm{h}} = \left( \sum_{i=1}^{N} \mathbf{V}_i \mathbf{V}_i^{\mathrm{T}} \right)^{+} \tag{80}$$

where $(.)^{+}$ indicates the pseudo inverse of the matrix, which is based on the singular value decomposition method. With $C_i$ in hand, the homogenous solution $\mathbf{u_h}$ in (40) can be rewritten as

$$\mathbf{u_h} = \mathrm{Re}\left\{ \left( \sum_{\mathrm{i}=1}^{\mathrm{N}} \frac{1}{s_i} \mathbf{h}_i e^{\alpha_i x + \beta_i y} \mathbf{V}_i^{\mathrm{T}} \right) \mathbf{R}_{\mathrm{h}} \bar{\mathbf{U}} \right\} \tag{81}$$

where $\mathrm{Re}\{.\}$ stands for the real part of the complex value.

It should be noted that some elements of $\mathbf{V}_i$ may contain the Young's modulus $E$, while the others may not. Thus, some elements may become extremely large, in comparison with others, and this may lead to some numerical errors in the evaluation of $\mathbf{R}_{\mathrm{h}}$ and also the rest of computations. To resolve this problem, we assume

$$\mathbf{V}_i = \mathbf{E}\tilde{\mathbf{V}}_i, \quad \bar{\mathbf{U}} = \mathbf{E}\tilde{\mathbf{U}} \tag{82}$$

where $\mathbf{E}$ is a diagonal matrix whose diagonal elements are equal to $Eh^3$ if their corresponding elements in $\mathbf{V}_i$ contain $E$, and are equal to one if else. For orthotropic materials the elasticity modulus in the direction normal to fiber directions is adopted as $E$.

Upon replacing $\bar{\mathbf{U}}$ and $\mathbf{V}_i$ in (73) with $\tilde{\mathbf{U}}$ and $\tilde{\mathbf{V}}_i$ defined in Equation (82), respectively, and conducting a procedure analogous to that which led to (80), one may find

$$C_i = \mathbf{V}_i^{\mathrm{T}} \mathbf{R}_{\mathrm{h}} \bar{\mathbf{U}}, \qquad \mathbf{R}_{\mathrm{h}} = \mathbf{E}^{-T} \left( \sum_{i=1}^{N} \tilde{\mathbf{V}}_i \tilde{\mathbf{V}}_i^{\mathrm{T}} \right)^{+} \mathbf{E}^{-1} \tag{83}$$

noting that $s_i$ defined in (78) will now be the norm of $\tilde{\mathbf{V}}_i$ instead of $\mathbf{V}_i$.

#### 4.2.1 Selection of $\alpha$ and $\beta$ for the homogenous part

Having discussed the procedure of constructing EBFs, we come to the point that one parameter in each pair of $(\alpha, \beta)$ must be selected arbitrarily, while the other one is deduced from the characteristic equation. The selection of $\alpha$ and $\beta$ affects the accuracy of the present method. In this regard, there are two strategies proposed by Boroomand et al. (2009), that we will overview both of them here and will employ the second one in Section 4. In some examples, a comparison between the results obtained by both strategies will also be given.

In both methods, $\alpha$ or $\beta$ are complex values picked from a feasible domain on the Gaussian-plane; that is

$$\alpha = a + b\ \mathbf{i}, \quad \beta = c + d\ \mathbf{i}, \qquad (a,\ b,\ c,\ d) \in \mathbb{R}^4 \tag{84}$$

In the case of choosing $\alpha$, the value of $b$ controls the periodic part and the value of $a$ determines the amplitude of the complex exponential in x-direction; and in the case of selecting $\beta$, similar definitions hold for $c$ and $d$ in y-direction. The pattern of choosing either $(a,\ b)$ for $\alpha$ or $(c,\ d)$ for $\beta$ will be described in two strategies, one based on mathematical reasoning and another based on numerical experiences.

*Strategy H1*

In this strategy $\alpha$ or $\beta$ are considered as pure imaginary values (i.e. $a = c = 0$). Assuming that $\beta$ is to be evaluated in terms of $\alpha$, the value of $b$ is to be selected manually. In this regard, one can put a limit on the value of $b$ by determining a reasonable number of oscillations between the boundary points, for example having at least a single oscillation within any sequence of four boundary point spaces. To this end, we define the average distant $\bar{d}_{avg}$ between adjacent points for representing the boundary point spacing as follows

$$\bar{d}_n = [(x_{n+1} - x_n)^2 + (y_{n+1} + y_n)^2]^{1/2}, \quad \bar{d}_{avg} = \frac{\sum_{n=1}^{M} \bar{d}_n}{M - 1} \simeq \frac{\sum_{n=1}^{M} \bar{d}_n}{M} \tag{85}$$

Now, by the assumption of occurring one oscillation on an interval of $4\bar{d}_n$, one may obtain the upper and lower bounds of $b$ along the imaginary axis of the Gaussian plane as

$$-\frac{\pi}{2\bar{d}_{avg}} \le b \le \frac{\pi}{2\bar{d}_{avg}} \qquad \text{when } \beta \text{ is evaluated in terms of } \alpha \tag{86}$$

and

$$-\frac{\pi}{2\bar{d}_{avg}} \le d \le \frac{\pi}{2\bar{d}_{avg}} \qquad \text{when } \alpha \text{ is evaluated in terms of } \beta \tag{87}$$

Having defined the feasible interval for $\alpha$ or $\beta$, a grid of points must be selected along this interval such that their corresponding basis functions have the most contributions to the solution. To this end, the maximum absolute value of the direct projection of these basis functions on the nodal boundary values may be calculated as follows

$$\begin{aligned} &P_{k_\alpha}^{\alpha} = \max(|\,(\mathbf{V}_{k_\alpha}^{\alpha,\beta_1})^T\ \bar{\mathbf{U}}\,|, |\,(\mathbf{V}_{k_\alpha}^{\alpha,\beta_2})^T\ \bar{\mathbf{U}}\,|, \ldots, |\,(\mathbf{V}_{k_\alpha}^{\alpha,\beta_r})^T\ \bar{\mathbf{U}}\,|) \\ &k_\alpha = 1,\ \ldots,\quad (\text{No. of grid points for } \alpha) \end{aligned} \tag{88}$$

and

$$P_{k_\beta}^{\beta} = \max(|(\mathbf{V}_{k_\beta}^{\alpha_1,\beta})^T\ \bar{\mathbf{U}}|, |(\mathbf{V}_{k_\beta}^{\alpha_2,\beta})^T\ \bar{\mathbf{U}}|, \ldots, |(\mathbf{V}_{k_\beta}^{\alpha_r,\beta})^T\ \bar{\mathbf{U}}|)$$
$$k_\beta = 1,\ \ldots,\quad (\text{No. of grid points for } \beta) \tag{89}$$

with $|\cdot|$ denoting the Hermitian length of the quantity. $\mathbf{V}_{k_\alpha}^{\alpha,\beta_j}$, $\mathbf{V}_{k_\beta}^{\alpha_j,\beta}$, $j = 1,\ \ldots,\ r$ represent the normalized vectors when the grids of $\alpha$ and $\beta$ are used, respectively; and $r$ denotes the number of basis functions found for each grid point through the characteristic equation. The maximum of the two series of numbers $P_{k_\alpha}^{\alpha}$ and $P_{k_\beta}^{\beta}$ are found as

$$P_{\max}^{\alpha} = \max_{k_\alpha}(P_{k_\alpha}^{\alpha}), \qquad P_{\max}^{\beta} = \max_{k_\beta}(P_{k_\beta}^{\beta}) \tag{90}$$

We choose all grid points whose projection values are greater than a specified value as $\xi$ times the maximum projections defined above, that is we choose $P_k$ so that

$$P_{k_\alpha}^{\alpha} \geq \xi \times P_{\max}^{\alpha}, \qquad P_{k_\beta}^{\beta} \geq \xi \times P_{\max}^{\beta}, \qquad 0<\xi<1 \tag{91}$$

*Strategy H2*

In this strategy the grids of points for $\alpha$, $\beta$ are defined in the form used in the work by Boroomand et al. (2009) for elasto-static problems. Based on our experience in the solution of plate bending problems for variety of simply connected domains with rather general shapes and various boundary conditions, again it has been found that the following form, for defining a suitable grid of points, works very well

$$\alpha = (a + b\ \mathbf{i}) = \pm \frac{\bar{m}\,\bar{\gamma}}{\bar{L}}\left(\frac{\bar{k}}{\bar{N}} + \mathbf{i}\right), \qquad \bar{m} = 1,\ \ldots,\ \bar{M},\ \ \bar{k} = 1,\ \ldots,\ \bar{N} \tag{92}$$

in which $\bar{M}, \bar{N} \in \mathbb{N}^2$, $\bar{\gamma} \in \mathbb{R}$ and $\bar{L}$ is a characteristic length. The following bounds are found to be appropriate in many cases

$$5.6 \leq \bar{\gamma} \leq 7.2\ (\text{say } \bar{\gamma} = 2\pi), \quad \bar{L} = 1.6 \max\left(L_x, L_y\right), \quad \bar{M}_{\min} = 4,\ \bar{N}_{\min} = 2,\ \bar{N}_{\max} = 8 \tag{93}$$

where $L_x$, $L_y$ are the dimensions of the rectangle circumscribing the whole domain as shown in Figure 2.a. A similar formula may be used for $\beta$. Although this formula is completely heuristic, it enables us to use a preliminary grid selection without putting too much effort on this part.

### 4.3 Particular solution

In this part we intend to find a particular solution $\mathbf{u_p}$ that satisfies

$$\mathbf{L u_p = q} \quad \text{in} \quad \Omega \tag{94}$$

where the differential operator $\mathbf{L}$ has been introduced in (19) or (20). Note that the particular solution may not satisfy the boundary conditions. In (Boroomand et al., 2009) two methods are proposed for finding the particular solution, we have adopted the one in which $\mathbf{u_p}$ is approximated by selecting another set of EBFs.

In this approach the plate loading $q(x\,,\,y)$ is approximated by a series of EBFs evaluated by a transformation technique similar to that introduced in Section 3.2. Therefore

$$q(x\,,y) = \sum_{k\,,l} g_{kl}\; e^{\alpha_k x + \beta_l y}\,, \qquad \forall (\mathrm{x,\ y}) \in \Omega \quad \text{and} \quad (\alpha_k\,,\beta_l) \in \mathbb{C}^2 \tag{95}$$

with

$$\alpha_k = a_k + b_k \mathbf{i}, \quad \beta_l = c_l + d_l \mathbf{i}, \qquad (a_k\,,b_k\,,c_l\,,d_l) \in \mathbb{R}^4 \tag{96}$$

where $\alpha_k\,,\beta_l$ are two independent complex values which are to be chosen in such a way that the determinant of the coefficient matrix in (35) does not vanish, that is

$$Det\ [\mathbf{L}_{(\alpha_k\,,\beta_l)}] \neq 0 \tag{97}$$

By considering a set of uniformly distributed points on the domain, defined by $L_x$ and $L_y$ in Figure 2.c, the constant coefficient $g_{k\,,l}$ can be found through the discrete transformation used earlier. Thus

$$g_{kl} = (\mathbf{V}_p)^T_{kl}\, \mathbf{R}_{\mathrm{p}} \bar{\mathbf{P}} \tag{98}$$

$$\mathbf{R}_{\mathrm{p}} = \left[ \sum_{k\,,l} (\mathbf{V}_p)_{kl}\, (\mathbf{V}_p)^T_{kl} \right]^{+} \tag{99}$$

$$\bar{\mathbf{P}} = \{ q(x_1, y_1)\ \ q(x_1, y_1)\ ....\ q(x_p, y_p)\ \}^T \tag{100}$$

$$(\mathbf{V}_p)_{kl} = \{ e^{\alpha_k x_1 + \beta_l y_1}\ \ e^{\alpha_k x_2 + \beta_l y_2}\ ....\ e^{\alpha_k x_p + \beta_l y_p}\ \}^T \tag{101}$$

where $p$ is the total number of grid points in the $L_x \times L_y$ domain. Note that the number of EBFs (i.e. $n_k + n_l$ ) is not necessarily equal to the number of domain points $p$ ; the number of $n_k\,,n_l$ may be increased until the loading $q(x\,,\,y)$ is approximated satisfactorily, which means that a discrete $\mathrm{L}_2$ norm becomes less than a specified value. Note that one may consider a larger

area for evaluation of $\mathbf{u_p}$, e.g. $1.1L_x \times 1.1L_y$, in order to have smooth variation of the function at the boundaries (see Boroomand et al. 2009).

The particular solution $\mathbf{u_p}$ is similarly represented in terms of exponential basis functions.

$$\mathbf{u}_{\mathrm{p}} = \sum_{k,l} \mathbf{h}_{kl}^{\mathrm{p}} \; e^{\alpha_k x + \beta_l y} \tag{102}$$

for FSDT and TSDT $\quad \mathbf{h}_{kl}^{\mathrm{p}} = \left\{ h_{kl}^{u},\ h_{kl}^{v},\ h_{kl}^{w},\ h_{kl}^{\phi_x},\ h_{kl}^{\phi_y} \right\}^T$

for CLPT $\quad \mathbf{h}_{kl}^{\mathrm{p}} = \left\{ h_{kl}^{u},\ h_{kl}^{v},\ h_{kl}^{w} \right\}^T$

Substitution of (95) and (102) into the governing equation (94) results in the following relation

$$\mathbf{L}_{kl}\mathbf{h}_{kl}^{\mathrm{p}} = \mathbf{c}_{kl}^{\mathrm{p}} \tag{103}$$

for FSDT and TSDT $\quad \mathbf{c}_{kl}^{\mathrm{p}} = \{0,\ 0,\ g_{kl},\ 0,\ 0\}^T$

for CLPT $\quad \mathbf{c}_{kl}^{\mathrm{p}} = \{0,\ 0,\ g_{kl}\}^T$

where, again, the constant coefficients of matrix $\mathbf{L}_{kl}$ can be obtained from those listed in Appendix A, with the following replacements

$$d_1^m = \alpha_k^m, \quad d_2^m = \beta_l^m \tag{104}$$

Note that in $\mathbf{c}_{kl}^{\mathrm{p}}$ defined above we have assumed that the laminated plate is just under transverse load $q(x, y)$ as in (95). In the case that in-plane loads act on the surface of the plate, the corresponding elements of $\mathbf{c}_{kl}^{\mathrm{p}}$ may take on non-zero values, however the procedure of finding them is similar to that of $g_{kl}$ explained above.

Upon solving the system of equations in (103), the unknown coefficients of vector $\mathbf{h}_{kl}^{\mathrm{p}}$ can be found in terms of $g_{kl}$ (or other similar factors) for each pair of $(\alpha_k,\ \beta_l)$. In the above formula, $\alpha_k$, $\beta_l$ are independent of each other and this means that they should be selected from two separate grids in Gaussian plane. Here, we suggest two strategies.

*Strategy P1*

In this case, we choose $\alpha_k$, $\beta_l$ as pure imaginary values, that is $a_k$, $c_k = 0$. Thus

$$\begin{aligned} &(\alpha_k, \beta_l) = (k\,\Delta b, l\,\Delta d)\mathbf{i}, && (\Delta b, \Delta d) \in (\mathbb{R}^+)^2 \\ &(k, l) \in \{-N_k, \ldots, -1, 0, 1, \ldots, N_k\} \cup \{-N_l, \ldots, -1, 0, 1, \ldots, N_l\}, && (N_k, N_l) \in (\mathbb{N})^2 \end{aligned} \tag{105}$$

where the integers $N_k, N_l$ as well as the spacing between the points $\Delta b, \Delta d$ are chosen in a way that convergence to the transverse load is satisfactorily achieved.

*Strategy P2*

In this case, we suggest a heuristic form for the grid points in the Gaussian plane for $\alpha_k$ , $\beta_l$ as follows

$$\begin{aligned}(\alpha_k, \beta_l) \in & \left\{\alpha = \pm\gamma_p (i + j\ \mathbf{i}), \alpha = \pm\gamma_p (i + j\ \mathbf{i}), i = 1,2,\ldots,n_p, j = 1,2,\ldots,n_p\right\} \\ & \cup\left\{\alpha = \pm\gamma_p (i + j\ \mathbf{i}), \alpha = \mp\gamma_p (i + j\ \mathbf{i}), i = 1,2,\ldots,n_p, j = 1,2,\ldots,n_p\right\} \\ & \cup\left\{\alpha = \pm\gamma_p (i + j\ \mathbf{i}), \alpha = \pm\gamma_p (j + i\ \mathbf{i}), i = 1,2,\ldots,n_p, j = 1,2,\ldots,n_p\right\} \\ & \cup\left\{\alpha = \pm\gamma_p (i + j\ \mathbf{i}), \alpha = \mp\gamma_p (j + i\ \mathbf{i}), i = 1,2,\ldots,n_p, j = 1,2,\ldots,n_p\right\} \\ & \cup\left\{\alpha = \pm\gamma_p (i + j\ \mathbf{i}), \alpha = \pm\gamma_p (i - j\ \mathbf{i}), i = 1,2,\ldots,n_p, j = 1,2,\ldots,n_p\right\} \\ & \cup\left\{\alpha = \pm\gamma_p (i + j\ \mathbf{i}), \alpha = \mp\gamma_p (i - j\ \mathbf{i}), i = 1,2,\ldots,n_p, j = 1,2,\ldots,n_p\right\} \\ & \cup\left\{\alpha = \pm\gamma_p (i + j\ \mathbf{i}), \alpha = \pm\gamma_p (j - i\ \mathbf{i}), i = 1,2,\ldots,n_p, j = 1,2,\ldots,n_p\right\} \\ & \cup\left\{\alpha = \pm\gamma_p (i + j\ \mathbf{i}), \alpha = \mp\gamma_p (j - i\ \mathbf{i}), i = 1,2,\ldots,n_p, j = 1,2,\ldots,n_p\right\}\end{aligned} \tag{106}$$

where $\gamma_p$ is defined as

$$\gamma_p = \frac{\kappa_p}{n_p \times \max(L_x, L_y)} \tag{107}$$

Based on our experience, we suggest the following values for $\kappa_p$ and $n_p$

$$\kappa_p = 12, \qquad n_p = 3 \tag{108}$$

The above formulation has been employed in variety of plate problems as well as other problems in elasticity and acoustics, in all of which convincing numerical results have been obtained.

*Remark 5*. In many plate problems $\mathbf{q}$ in (94) is expressed as a simple functions such as polynomials and trigonometric functions. In such cases the particular solution may be found explicitly which of course is not unique. For instance in CLPT when the plate is under uniform load, the particular solution may be considered as the particular solution in a Bernoulli beam (as function of $x$ or $y$ ). In this report we have treated the loadings as the general ones and used the afore-mentioned procedure to find the particular solutions.

## 5. NUMERICAL RESULTS

Here, we apply the presented procedure for solving a number of bending problems of both single layer and multilayered plates with different domain geometries, loadings and boundary conditions. In this regard, the following material properties have been considered

Orthotropic material:

$$E_2 = E_3 = 10\text{GPa}, \quad E_1 = 25E, \quad G_{12} = G_{13} = 0.5E, \quad G_{23} = 0.2E, \quad \nu_{12} = \nu_{23} = \nu_{13} = 0.25, \tag{109}$$

Isotropic material:

$$E = 30\text{GPa}, \quad G = E/2(1+\nu), \quad D = Eh^3/12(1-\nu^2), \quad \nu = 0.3 \tag{110}$$

### 5.1. Square plates

Consider a square plate with side length $a$ and thickness of $h$ as shown in Figure 3. The upper surface of the plate is subjected to a sinusoidally distributed transverse load as follows

$$q(x_1, x_2) = q_0 \cos(\frac{\pi x_1}{a}) \cos(\frac{\pi x_2}{a}) \tag{111}$$

where $q_0 = 100$ kPa is the maximum load intensity.

Here, the values of bending deflection and stresses of laminated plates with two forms of layups and various boundary conditions will be investigated. The results will be given in terms of the following non-dimensional forms

$$\begin{aligned}
&\bar{u}_3 = \frac{100h^3 E_2}{q_0 a^4} \bar{u}_3(0,0), \\
&\bar{\sigma}_{11}^{(m)} = \frac{h^2}{q_0 a^2} \sigma_{11}(0,0,x_3), \quad \bar{\sigma}_{22}^{(m)} = \frac{h^2}{q_0 a^2} \sigma_{22}(0,0,x_3), \quad \bar{\sigma}_{12}^{(m)} = \frac{h^2}{q_0 a^2} \sigma_{12}(a,a,x_3), \\
&\bar{\sigma}_{23}^{(m)} = \frac{h}{q_0 a} \sigma_{23}(0,-a/2,x_3), \qquad \bar{\sigma}_{13}^{(m)} = \frac{h}{q_0 a} \sigma_{13}(-a/2,0,x_3),
\end{aligned} \tag{112}$$

where the superscript $m$ indicates the layer number, as shown in Figure 1.

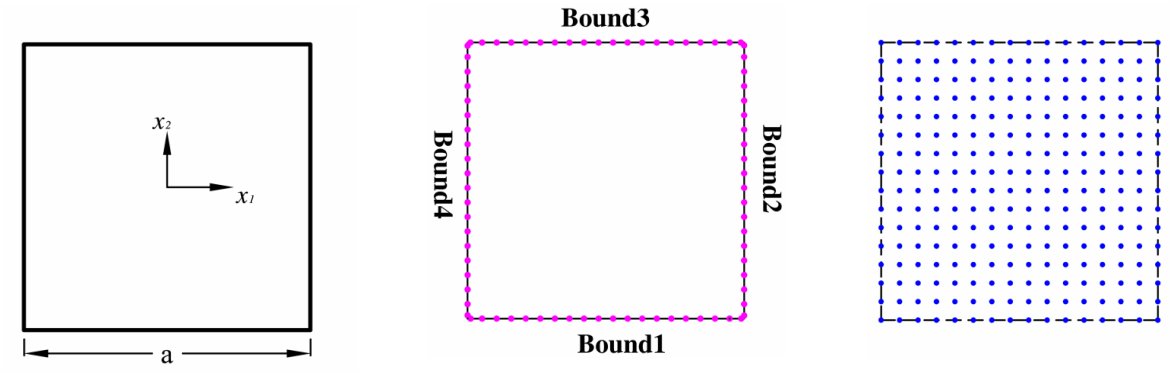


***Figure 3. The plate domain: (a) Plate geometry and sequence of boundary edges numbering; (b) Boundary points; (c) Distribution of domain points for construction of*** $\mathbf{u}_p$ ***.***

Table 2 shows the center deflection, in-plane stresses and transverse shear stresses of a simply supported symmetric cross-ply $(0^o,90^o,90^o,0^o)$ square plate $(a=20\text{m})$, with various side-to-thickness ratios using FSDT, TSDT and CLPT. The numerical results are compared to the exact ones obtained by the Navier solution in (Reddy, 2004). As shown in Figure 3, the boundary of the plate is discretized by $M=80$ evenly spaced points (i.e. 20 points along each side), for imposing the boundary conditions; while a regular grid of $16\times16$ is considered on the domain (i.e. $P=256$), at which the particular solution is found. Worthwhile to mention that, at the corners of the plate, we have used two separate closely spaced points at the two intersecting boundaries.

**Table 2. The non-dimensional deflection and stresses of a simply supported four-layer symmetric cross-ply (0 °, 90 °, 90 °,0 °) laminated plate under sinusoidally distributed transverse load.**

| a/h | Method | $\bar{u}_3$ | $\bar{\sigma}_{11}^{(4)}(h/2)$ | $\bar{\sigma}_{22}^{(2)}(h/4)$ | $\bar{\sigma}_{12}^{(1)}(-h/2)$ | $\bar{\sigma}_{23}^{(2)}(0)$ | $\bar{\sigma}_{13}^{(2)}(0)$ |
|---|---|---|---|---|---|---|---|
| 10 | FSDT | 0.66271 | 0.49888 | 0.36142 | 0.02411 | 0.12918 | 0.16660 |
| | | (0.66271) | (0.49888) | (0.36142) | (0.02413) | (0.12918) | (0.16660) |
| | TSDT | 0.71474 | 0.54558 | 0.38880 | 0.02666 | 0.15310 | 0.26402 |
| | | (0.71474) | (0.54558) | (0.38880) | (0.02676) | (0.15305) | (0.26400) |
| 20 | FSDT | 0.49117 | 0.52733 | 0.29565 | 0.02206 | 0.10865 | 0.17481 |
| | | (0.49117) | (0.52732) | (0.29565) | (0.02210) | (0.10869) | (0.17490) |
| | TSDT | 0.50604 | 0.53928 | 0.30429 | 0.02286 | 0.12304 | 0.28244 |
| | | (0.50604) | (0.53928) | (0.30429) | (0.02280) | (0.12341) | (0.28249) |
| 100 | FSDT | 0.43368 | 0.53822 | 0.27045 | 0.02130 | 0.10086 | 0.17794 |
| | | (0.43367) | (0.53822) | (0.27045) | (0.02132) | (0.10083) | (0.17794) |
| | TSDT | 0.43430 | 0.53870 | 0.27082 | 0.02142 | 0.12453 | 0.29980 |
| | | (0.43430) | (0.53870) | (0.27083) | (0.02134) | (0.11168) | (0.28972) |
| | CLPT | 0.43125 | 0.53870 | 0.26935 | 0.02128 | 0.13819[b] | 0.33927[b] |
| | | (0.43125) | (0.53870) | (0.26935) | (0.02128) | (0.13820)[b] | (0.33927)[b] |

[a] The values in parentheses are from the exact Navier solutions due to (Reddy, 2004).

[b] These values are evaluated from equilibrium equations at $x_3=0$.

For the homogenous solution, we have used strategy H2 with $\bar{\gamma} = 2\pi$ and $\bar{M} = \bar{N} = 3$ that gives total numbers of 144, 216, 288 EBFs, respectively, for CLPT, FSDT and TSDT. The particular response has been found by strategy P1 with 288 basis functions from (106) by setting $\kappa_p = 12$ and $n_p = 3$. As is seen in Table 1, excellent accuracy is obtained in all cases. For CLPT we have calculated shear stresses at mid-plane through equilibrium equations. Again excellent agreement is seen between the numerical and the exact solutions.

Table 3 compares the results for a moderately thick square plate $(a/h = 20)$ obtained through strategy H1 and H2 for the homogenous solution. In strategy H1, a series of numbers have been chosen along the imaginary axis in Gaussian plane, for which the variations of parameters $P^{\alpha}_{k_\alpha}$ and $P^{\beta}_{k_\beta}$, defined in (88) and (89), are shown in Figure 4 (for FSDT as an example). By selecting $\zeta = 0.2$, the following values are obtained for $\alpha$ and $\beta$

$$\alpha = b\ \mathbf{i}, \quad b \in \{[-0.5, -\varepsilon] \cup [\varepsilon, 0.5]\}, \ \Delta b = 0.05, \ \ \varepsilon = 0.01 \tag{113}$$

and

$$\beta = d\ \mathbf{i}, \quad d \in \{[-0.5, -\varepsilon] \cup [\varepsilon, 0.5]\}, \ \Delta d = 0.05, \ \ \varepsilon = 0.01 \tag{114}$$

As a result, the total number of EBFs in this strategy amounts to 240. Conducting a similar procedure for TSDT yields 256 EBFs. As is seen in Table 2, the estimated errors in both strategies are nearly the same.

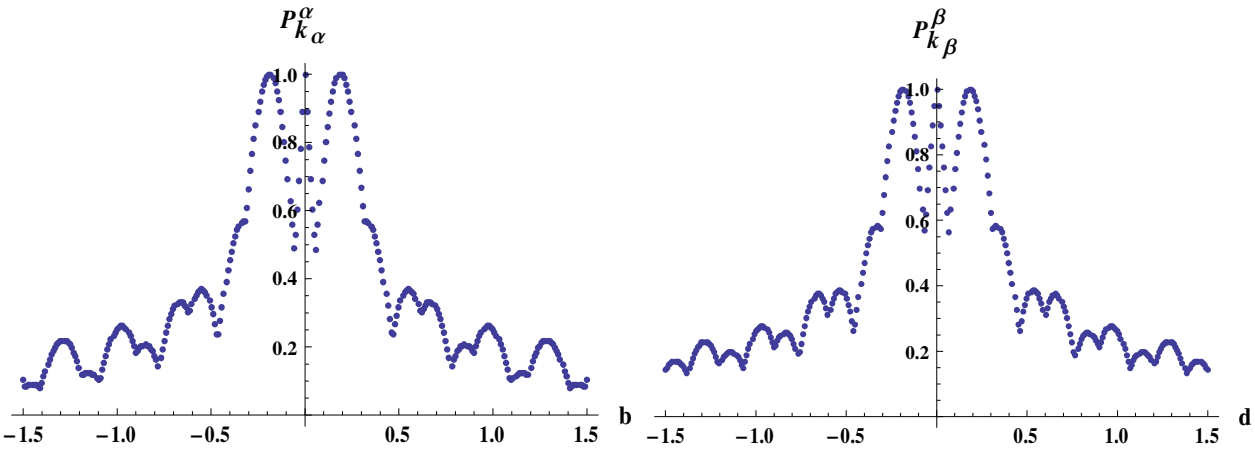


***(a)*** ***(b)***

***Figure 4. Variations of parameters*** $P^{\alpha}_{k_\alpha}$ ***and*** $P^{\beta}_{k_\beta}$ ***, for a simply supported cross-ply (0°,90°,90°,0°) laminated plate under sinusoidally distributed transverse load with*** $(a/h = 20)$ ***: (a) Variations of*** $P^{\alpha}_{k_\alpha}$ ***; (b) Variations of*** $P^{\beta}_{k_\beta}$

**Table 3. The absolute errors of the quantities in Table 2 obtained by strategies H1 and H2 in solution of a simply supported cross-ply ($0^o$,$90^o$, $90^o$,$0^o$) laminated plate under sinusoidal load** $(a/h = 20)$ **. The errors are in percent.**

| Method | $\eta_{\bar{u}_3}\%$ | $\eta_{\bar{\sigma}_{11}}\%$ | $\eta_{\bar{\sigma}_{22}}\%$ | $\eta_{\bar{\sigma}_{12}}\%$ | $\eta_{\bar{\sigma}_{23}}\%$ | $\eta_{\bar{\sigma}_{13}}\%$ |
|---|---|---|---|---|---|---|
| FSDT-H1 | 0.000670 | 0.000443 | 0.000152 | 0.315217 | 0.000808 | 0.009644 |
| FSDT-H2 | 0.000038 | 0.000440 | 0.000602 | 0.173877 | 0.0312426 | 0.005550 |
| TSDT-H1 | 0.000165 | 0.000316 | 0.000097 | 1.29610 | 0.585785 | 0.036924 |
| TSDT-H2 | 0.000019 | 0.000010 | 0.000139 | 0.284110 | 0.297711 | 0.01489 |

Table 4 shows the non-dimensional deflections and stresses of a simply supported symmetric cross-ply ($0^o$,$90^o$,$0^o$) square plate subjected to a uniformly distributed transverse load. We have used strategy H2 and the number boundary points, domain grid points and basis functions are the same as those in the previous problem. Here again excellent agreement is seen between the obtained results and those of the exact solution given in (Reddy, 2004), especially for the center deflection and the normal bending stresses. For shear stress resultants at the mid points of the edges, some discrepancies are seen between the two sets of results; however, the errors are very small considering the order of the original non-normalized values (see Equation (112)).

It should be noted that in a symmetric cross-ply the in-plane forces are identically zero since there is no coupling between the in-plane displacements and the bending displacements. In this regard, we can use the simplified form of the differential equations given in (20) for analysis of symmetric laminated plates.

**Table 4. The non-dimensional deflection and stresses of a simply supported three-layer symmetric cross-ply ($0^o$, $90^o$ , $0^o$) laminated plate under uniformly distributed transverse load.**

| a/h | Method | $\bar{u}_3$ | $\bar{\sigma}_{11}^{(3)}(h/2)$ | $\bar{\sigma}_{22}^{(2)}(h/6)$ | $\bar{\sigma}_{12}^{(1)}(-h/2)$ | $\bar{\sigma}_{23}^{(2)}(0)$ | $\bar{\sigma}_{13}^{(3)}(h/6)$ |
|---|---|---|---|---|---|---|---|
| 10 | FSDT | 1.02188 | 0.77189 | 0.30744 | 0.05042 | 0.33110 | 0.77033 |
| | | (1.02188) | (0.77187) | (0.30722) | (0.05138) | (0.31075) | (0.75486) |
| | TSDT | 1.08977 | 0.83902 | 0.33453 | 0.05657 | 0.34841 | 0.98002 |
| | | (1.08992) | (0.83853) | (0.33464) | (0.05905) | (0.34059) | (0.978266) |
| 20 | FSDT | 0.75722 | 0.79834 | 0.222961 | 0.04505 | 0.31019 | 0.78537 |
| | | (0.75723) | (0.79832) | (0.22274) | (0.04528) | (0.29019) | (0.76970) |
| | TSDT | 0.77597 | 0.81603 | 0.23077 | 0.04867 | 0.33101 | 1.03235 |
| | | (0.77595) | (0.81566) | (0.23065) | (0.04744) | (0.31651) | (1.02730) |
| 100 | FSDT | 0.66969 | 0.80721 | 0.19273 | 0.04281 | 0.30444 | 0.79034 |
| | | (0.66969) | (0.80717) | (0.19251) | (0.04265) | (0.28421) | (0.77446) |
| | TSDT | 0.67046 | 0.80794 | 0.19305 | 0.04280 | 0.30814 | 1.06622 |
| | | (0.67047) | (0.80787) | (0.19284) | (0.04275) | (0.30958) | (1.04704) |
| | CLPT | 0.66601 | 0.80758 | 0.19143 | 0.04241 | 0.40770[b] | 0.73395[b] |
| | | (0.66601) | (0.80753) | (0.19122) | (0.04252) | (0.37906)[b] | (0.71912)[b] |

[a] The values in parentheses are from the exact Navier solutions due to (Reddy, 2004).

[b] These values are evaluated from equilibrium equations at $x_3 = 0$

Table 5-8 contain the non-dimensional deflection and stresses of an anti-symmetric cross-ply ($0^o$,$90^o$) square plate under a sinusoidal load with various boundary conditions and side-to-thickness ratios. In order to specify the boundary conditions of the plate, we have used the numbering sequence shown in Figure 3.a. For instance, SCSF denotes a plate with simply supported edges on the boundaries 1 and 3, clamped on the boundary 2 and free on the edge 4.

In this problem, the boundary and domain grid points have been adopted similar to the previous problems. Although we have selected $\bar{\gamma} = 2\pi$ and $\bar{M} = \bar{N} = 3$, the number of EBFs for this problem will increase to 288, 360 and 432. This is a result of the larger number of roots that one can find from the characteristic equation of an antisymmetric laminate in comparison with that of a symmetric laminate. All the results have been compared to the exact Levy solutions available in (Khdeir and Reddy, 1991). We have reported the exact values with the decimal part given in the reference; however, for the numerical results we have reported values with more precision. Again, excellent agreement is seen between the two sets of results. Note that in anti-symmetric angle-ply or cross-ply laminates, we have to deal with the complete form of the differential equations given in (19) since the bending and extension displacements are coupled.

**Table 5. Non-dimensional center deflection $\bar{u}_3$ of an anti-symmetric cross-ply ($0^o$,$90^o$) laminated plate under sinusoidally distributed transverse load.**

| a/h | Theory | Method | SSSS | SSSC | SCSC | SFSF | SFSS | SFSC |
|---|---|---|---|---|---|---|---|---|
| 5 | FSDT | Reference[a] | 1.758 | 1.477 | 1.257 | 2.777 | 2.335 | 1.897 |
| | | Present | 1.75835 | 1.47704 | 1.25654 | 2.77699 | 2.33456 | 1.89712 |
| | TSDT | Reference[a] | 1.667 | 1.333 | 1.088 | 2.624 | 2.211 | 1.733 |
| | | Present | 1.66695 | 1.33282 | 1.08756 | 2.62409 | 2.21087 | 1.73279 |
| 10 | FSDT | Reference[a] | 1.237 | 0.883 | 0.656 | 2.028 | 1.687 | 1.223 |
| | | Present | 1.23727 | 0.882869 | 1.25654 | 2.02813 | 1.68722 | 1.22256 |
| | TSDT | Reference[a] | 1.216 | 0.848 | 0.617 | 1.992 | 1.658 | 1.184 |
| | | Present | 1.21612 | 0.848421 | 0.616791 | 1.99216 | 1.65825 | 1.18421 |
| | CLPT | Reference[a] | 1.06358 | 0.664 | 0.429 | 1.777 | 1.471 | 0.980 |
| | | Present | 1.06358 | 0.66367 | 0.428979 | 1.77652 | 1.47083 | 0.980202 |

[a] (Khdeir and Reddy, 1991)

**Table 6. Non-dimensional in-plane stress $-\bar{\sigma}_{11}^{(1)}(-h/2)$ of an anti-symmetric cross-ply ($0^o$,$90^o$) laminated plate under sinusoidally distributed transverse load.**

| a/h | Theory | Method | SSSS | SSSC | SCSC | SFSF | SFSS | SFSC |
|---|---|---|---|---|---|---|---|---|
| 5 | FSDT | Reference[a] | 0.7157 | 0.5338 | 0.3911 | 0.2469 | 0.4430 | 0.2434 |
| | | Present | 0.715746 | 0.533814 | 0.391052 | 0.246901 | 0.442978 | 0.24339 |
| | TSDT | Reference[a] | 0.8385 | 0.6816 | 0.5679 | 0.3171 | 0.5349 | 0.3727 |
| | | Present | 0.838548 | 0.681644 | 0.567871 | 0.317091 | 0.534857 | 0.372681 |
| 10 | FSDT | Reference[a] | 0.7157 | 0.5494 | 0.4450 | 0.2442 | 0.4435 | 0.2790 |
| | | Present | 0.715745 | 0.549383 | 0.445049 | 0.244192 | 0.443501 | 0.279037 |
| | TSDT | Reference[a] | 0.7468 | 0.5910 | 0.4952 | 0.2624 | 0.4669 | 0.3158 |
| | | Present | 0.74679 | 0.590994 | 0.495244 | 0.262496 | 0.466969 | 0.315784 |
| | CLPT | Reference[a] | 0.715745 | 0.5660 | 0.4800 | 0.2403 | 0.4442 | 0.3042 |
| | | Present | 0.715746 | 0.565662 | 0.477584 | 0.240269 | 0.444158 | 0.303855 |

[a] (Khdeir and Reddy, 1991)

**Table 7. Non-dimensional in-plane stress $\bar{\sigma}_{22}^{(2)}(h/2)$ of an anti-symmetric cross-ply ($0^o$,$90^o$) laminated plate under sinusoidally distributed transverse load.**

| a/h | Theory | Method | SSSS | SSSC | SCSC | SFSF | SFSS | SFSC |
|---|---|---|---|---|---|---|---|---|
| 5 | FSDT | Reference[a] | 0.7157 | 0.6034 | 0.5153 | 1.1907 | 0.9848 | 0.8047 |
| | | Present | 0.715744 | 0.603354 | 0.515255 | 1.19071 | 0.984794 | 0.804679 |
| | TSDT | Reference[a] | 0.8385 | 0.6725 | 0.5505 | 1.3551 | 1.1324 | 0.8919 |
| | | Present | 0.838546 | 0.672454 | 0.550484 | 1.3552 | 1.13238 | 0.891852 |
| 10 | FSDT | Reference[a] | 0.7157 | 0.5109 | 0.3799 | 1.1884 | 0.9847 | 0.7150 |
| | | Present | 0.715747 | 0.510852 | 0.379918 | 1.18839 | 0.984706 | 0.715028 |
| | TSDT | Reference[a] | 0.7468 | 0.5219 | 0.3803 | 1.2295 | 1.0218 | 0.7314 |
| | | Present | 0.746792 | 0.521916 | 0.380322 | 1.22948 | 1.02183 | 0.731365 |
| | CLPT | Reference[a] | 0.715745 | 0.4483 | 0.2914 | 1.1849 | 0.9837 | 0.6560 |
| | | Present | 0.715743 | 0.448264 | 0.291284 | 1.18487 | 0.983728 | 0.656008 |

[a] (Khdeir and Reddy, 1991)

**Table 8. Non-dimensional transverse shear stress $\bar{\sigma}_{23}^{(2)}(0)$ of an anti-symmetric cross-ply ($0^o$,$90^o$) laminated plate under sinusoidally distributed transverse load.**

| a/h | Theory | Method | SSSS | SSSC | SCSC | SFSF | SFSS | SFSC |
|---|---|---|---|---|---|---|---|---|
| 5 | FSDT | Reference[a] | 0.2729 | 0.2297 | 0.1958 | 0.3901 | 0.3390 | 0.2748 |
| | | Present | 0.272846 | 0.229659 | 0.195799 | 0.390105 | 0.339034 | 0.274787 |
| | TSDT | Reference[a] | 0.3155 | 0.2543 | 0.2095 | 0.4457 | 0.3893 | 0.3048 |
| | | Present | 0.31544 | 0.254293 | 0.20947 | 0.445688 | 0.389311 | 0.304752 |
| 10 | FSDT | Reference[a] | 0.2729 | 0.1993 | 0.1523 | 0.3882 | 0.3383 | 0.2449 |
| | | Present | 0.272844 | 0.199272 | 0.152292 | 0.388215 | 0.338265 | 0.244953 |
| | TSDT | Reference[a] | 0.3190 | 0.2290 | 0.1725 | 0.4489 | 0.3927 | 0.2805 |
| | | Present | 0.319027 | 0.22906 | 0.17247 | 0.448907 | 0.392784 | 0.280471 |

[a] (Khdeir and Reddy, 1991)

## 5.2. Annular plates

Consider an isotropic $60^o$ annular sector plate with outer radius $r_{out} = a = 20\text{m}$, inner radius $r_{in} = b = 10\text{m}$ and a constant thickness $h$, as shown in Figure 5, subjected to a uniformly distributed transverse load with $q_0 = 50\,\text{kPa}$ intensity.

In this problem the non-dimensional deflection, bending moment resultants and transverse shearing force resultants have been calculated at six points of the plate with respect to the polar-coordinate system shown in Figure 5, similar to those in (Kobayashi and Turvey, 1994): point a $(r = a, \theta = 0)$, point b $(r = (a+b)/2,\ \theta = 0)$, point c $(r = b, \theta = 0)$, point d $(r = a, \theta = \alpha/2)$, point e $(r = (a+b)/2, \theta = \alpha/2)$ and point f $(r = b, \theta = \alpha/2)$. The non-dimensional values are as follows

$$\bar{u}_3 \left(= \frac{10^3 D}{q_0 c^4} u_3\right), \quad \bar{Q}_r \left(= \frac{1}{q_0 c} Q_r\right), Q_\theta$$
$$\bar{M}_{rr} \left(= \frac{10^2}{q_0 c^2} M_{rr}\right), \bar{M}_{\theta\theta}, \bar{M}_{r\theta} \tag{115}$$

where $c = b - a$ .

Table 9-11 contain the above-mentioned values for a SSSS, SCSC and SFSF plates, respectively, considering various plate thicknesses $h/c$ . The analytical solutions based on FSDT and CLPT obtained by Kobayashi and Turvey (1994) are also tabulated for comparison.

As is seen in Figs. 5.b and 5.c, a total number of 50 evenly spaced points are taken along the edges of the plate and a grid of 18×31 are chosen in the rectangle circumscribing the plate domain. The number of exponential basis functions for solving the homogenous and particular parts is the same as that of the previous problems.

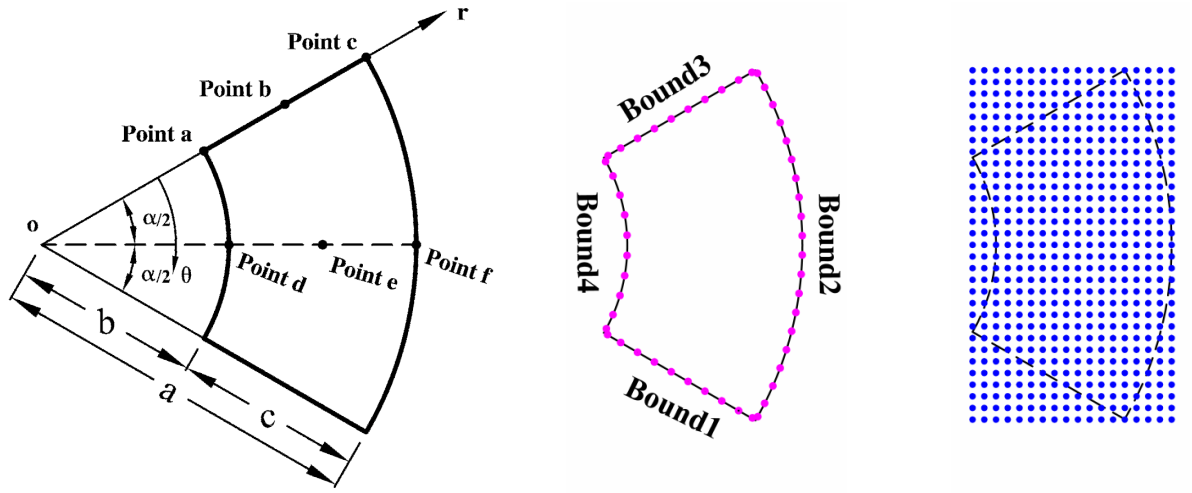


***Figure 5. The plate domain: (a) plate geometry; (b) Boundary points and sequence of boundary edges numbering; (c) Distribution of domain points.***

For SSSS plates, it can be seen in Table 9 that the presented results are in excellent agreement with those given in the reference, especially for the deflections and extensional bending moment resultants. Very small discrepancies can be seen between the two sets of results for shear stress resultants and the twisting moments. As expected, the results of FSPT approach those of CLTP as $h/c$ decreases. Similar conclusions may be made from Table 10 for plates with SCSC condition.

The results of plates with SFSF condition are given in Table 11. Due to the presence of free boundaries, we present two sets of results, one obtained from the application of the boundary

conditions listed in Table 1 for free boundaries (denoted by superscript "b") and another obtained from the application of the conditions suggested in Remark 1(denoted by superscript "c").

For plates with $h/c$ between 0.1 to 0.2 the two sets of results are in good agreement with those given in Kobayashi and Turvey (1994). As $h/c$ becomes less than 0.05, the discrepancy between the results obtained by the boundary conditions in Table 1 and the other two grows dramatically. The reason lies in the fact that when the boundary condition of Table 1 are applied, strong singularity effect is seen in twisting moment and shear stress resultants at corners (see Kobayashi and Turvey 1994). The effect becomes prominent when a very small plate thickness is chosen. In order to take into account such singularity effect in the presented method, one should add a set of appropriate EBFs to the former set. The discussion is beyond the scope of this report (see Boroomand and Mossaiby 2006 for the use of EBFs obtained from FEM for construction of singular discrete Green's functions).

Such strong singularity is not seen in the boundary conditions used in CLPT since in Kirchhoff's shear resultant the twisting moment and the shear resultant are combined (see Remark 1). From the results denoted by superscript "c" in Table 11, it can be seen that one may overcome the effect by defining boundary conditions given in (22) without changing the bases. As is seen in the table, the deflections and stress resultants smoothly approach to their counterparts in CLPT when the thickness of the plate decreases. For instance comparison of the results for h/c=0.01 obtained by FSDT with those obtained by CLPT shows excellent agreement.

**Table 9. Non-dimensional deflection, moment resultants and transverse shear stress resultants for a uniformly loaded SSSS isotropic annular sector plate** $(a/b=0.5,\ \alpha=60^\circ)$**.**

| Theory | h/c | Method | $\bar{u}_3^e$ | $\bar{M}_{rr}^e$ | $\bar{M}_{\theta\theta}^e$ | $\bar{M}_{r\theta}^a$ | $\bar{M}_{r\theta}^c$ | $\bar{Q}_r^d$ | $\bar{Q}_r^f$ | $\bar{Q}_\theta^b$ |
|---|---|---|---|---|---|---|---|---|---|---|
| FSDT | 0.20 | Reference[a] | 9.1917 | 8.3669 | 4.8948 | -6.4498 | 3.2907 | 0.5279 | -0.3848 | 0.3622 |
| | | Present | 9.1918 | 8.3669 | 4.8948 | -6.4500 | 3.2931 | 0.5281 | -0.3847 | 0.3633 |
| | 0.15 | Reference[a] | 8.6716 | 8.3696 | 4.8851 | -6.4179 | 3.3021 | 0.5304 | -0.3845 | 0.3621 |
| | | Present | 8.6716 | 8.3696 | 4.8851 | -6.4253 | 3.2907 | 0.5305 | -0.3846 | 0.3631 |
| | 0.10 | Reference[a] | 8.2998 | 8.3715 | 4.8779 | -6.3703 | 3.3170 | 0.5328 | -0.3843 | 0.3620 |
| | | Present | 8.2999 | 8.3715 | 4.8780 | -6.3874 | 3.3252 | 0.53280 | -0.3842 | 0.3629 |
| | 0.05 | Reference[a] | 8.0765 | 8.3725 | 4.8735 | -6.3044 | 3.3361 | 0.5352 | -0.3840 | 0.3620 |
| | | Present | 8.0775 | 8.3733 | 4.8741 | -6.3829 | 3.4218 | 0.5344 | -0.3836 | 0.3628 |
| | 0.02 | Reference[a] | 8.0140 | 8.3728 | 4.8722 | -6.2551 | 3.3497 | 0.5366 | -0.3839 | 0.3620 |
| | | Present | 8.0144 | 8.3731 | 4.8725 | -6.3226 | 3.0736 | 0.5371 | -0.3857 | 0.3632 |
| | 0.01 | Reference[a] | 8.0051 | 8.3729 | 4.8720 | -6.2369 | 3.3547 | 0.5370 | -0.3838 | 0.3620 |
| | | Present | 8.0051 | 8.3729 | 4.8721 | -6.2846 | 3.5021 | 0.5375 | -0.3819 | 0.3630 |
| CLPT | 0.00 | Reference[a] | 8.0021 | 8.3729 | 4.8719 | -6.2177 | 3.3599 | 0.5375 | -0.3838 | 0.3620 |
| | | Present | 8.0021 | 8.3729 | 4.8719 | -6.1707 | 3.3198 | 0.5374 | -0.3835 | 0.3627 |

[a] (Kobayashi and Turvey, 1994)

**Table 10. Non-dimensional deflection, moment resultants and transverse shear stress resultants for a uniformly loaded SCSC isotropic annular sector plate** $(a/b = 0.5,\ \alpha = 60^\circ)$**.**

| Theory | h/c | Method | $\bar{u}_3^e$ | $\bar{M}_{rr}^e$ | $\bar{M}_{\theta\theta}^e$ | $\bar{M}_{r\theta}^a$ | $\bar{M}_{r\theta}^c$ | $\bar{Q}_r^d$ | $\bar{Q}_r^f$ | $\bar{Q}_\theta^b$ |
|---|---|---|---|---|---|---|---|---|---|---|
| FSDT | 0.20 | Reference[a] | 3.9744 | 4.1445 | 2.0465 | -2.1088 | 1.1836 | 0.6381 | -0.4598 | 0.2469 |
| | | Present | 3.9744 | 4.1444 | 2.04651 | -2.1067 | 1.1667 | 0.6382 | -0.4598 | 0.2478 |
| | 0.15 | Reference[a] | 3.3508 | 4.1276 | 1.9210 | -1.7173 | 0.94741 | 0.6508 | -0.4585 | 0.2437 |
| | | Present | 3.3508 | 4.1275 | 1.9210 | -1.7081 | 0.93949 | 0.6508 | -0.4585 | 0.2447 |
| | 0.10 | Reference[a] | 2.8955 | 4.1089 | 1.8266 | -1.2524 | 0.68063 | 0.6603 | -0.4569 | 0.2411 |
| | | Present | 2.8955 | 4.1089 | 1.8266 | -1.2515 | 0.67910 | 0.6601 | -0.4569 | 0.2421 |
| | 0.05 | Reference[a] | 2.6167 | 4.0935 | 1.7688 | -0.6900 | 0.37161 | 0.6659 | -0.4557 | 0.2391 |
| | | Present | 2.6163 | 4.0930 | 1.7690 | -0.7084 | 0.36836 | 0.6682 | -0.4566 | 0.2404 |
| | 0.02 | Reference[a] | 2.5375 | 4.0881 | 1.7526 | -0.2928 | 0.15810 | 0.6686 | -0.4556 | 0.2384 |
| | | Present | 2.5373 | 4.0881 | 1.7523 | -0.3006 | 0.15796 | 0.6702 | -0.4565 | 0.2388 |
| | 0.01 | Reference[a] | 2.5261 | 4.0873 | 1.7503 | -0.1491 | 0.08085 | 0.6697 | -0.4556 | 0.2383 |
| | | Present | 2.5261 | 4.0873 | 1.7501 | -0.1490 | 0.08092 | 0.6717 | -0.4562 | 0.2382 |
| CLPT | 0.00 | Reference[a] | 2.5223 | 4.0870 | 1.7495 | 0 | 0 | 0.6708 | -0.4555 | 0.2383 |
| | | Present | 2.5223 | 4.0870 | 1.74947 | 0.00054 | 0.00013 | 0.6710 | -0.4561 | 0.2398 |

**Table 11. Non-dimensional deflection, moment resultants and transverse shear stress resultants for a uniformly loaded SFSF isotropic annular sector plate** $(a/b = 0.5,\ \alpha = 60^\circ)$**.**

| Theory | h/c | Method | $\bar{u}_3^d$ | $\bar{u}_3^e$ | $\bar{u}_3^f$ | $\bar{M}_{rr}^e$ | $\bar{M}_{\theta\theta}^d$ | $\bar{Q}_\theta^a$ | $\bar{Q}_\theta^b$ | $\bar{Q}_\theta^c$ |
|---|---|---|---|---|---|---|---|---|---|---|
| FSDT | 0.20 | Reference[a] | 61.915 | 132.12 | 230.01 | 0.85269 | 42.003 | -0.5520 | 0.7340 | 2.622 |
| | | Present[b] | 61.930 | 132.14 | 230.05 | 0.85220 | 41.966 | -0.5425 | 0.7349 | 2.625 |
| | | Present[c] | 62.107 | 132.08 | 229.91 | 0.8280 | 41.515 | -0.7680 | 0.7352 | 2.655 |
| | 0.15 | Reference[a] | 61.145 | 129.97 | 226.27 | 0.97760 | 41.484 | -0.9716 | 0.7350 | 3.217 |
| | | Present[b] | 61.123 | 129.90 | 226.13 | 0.98064 | 41.390 | -0.9504 | 0.7360 | 3.196 |
| | | Present[c] | 61.692 | 129.84 | 225.84 | 0.8907 | 40.774 | -0.8459 | 0.7341 | 3.193 |
| | 0.10 | Reference[a] | 60.704 | 128.28 | 223.10 | 1.1043 | 40.996 | -1.818 | 0.7363 | 4.406 |
| | | Present[b] | 60.647 | 128.13 | 222.80 | 1.1130 | 40.762 | -1.701 | 0.7380 | 4.383 |
| | | Present[c] | 61.807 | 127.92 | 221.95 | 0.9348 | 40.102 | 1.1133 | 0.7362 | 2.426 |
| | 0.05 | Reference[a] | 60.596 | 127.06 | 220.51 | 1.2312 | 40.537 | -4.368 | 0.7377 | 7.972 |
| | | Present[b] | 45.470 | 85.020 | 137.10 | 3.9654 | 31.273 | -0.607 | 0.6314 | 16.598 |
| | | Present[c] | 61.01 | 126.22 | 216.91 | 1.6082 | 40.115 | 1.0939 | 0.7394 | 0.6252 |
| | 0.02 | Reference[a] | 60.691 | 126.55 | 219.23 | 1.3069 | 40.274 | -12.03 | 0.7385 | 18.67 |
| | | Present[b] | 36.224 | 60.627 | 87.225 | 6.1287 | 25.692 | -0.155 | 0.5700 | 4.422 |
| | | Present[c] | 60.850 | 126.32 | 218.50 | 1.3572 | 40.099 | 0.9932 | 0.7405 | 0.5541 |
| | 0.01 | Reference[a] | 60.750 | 126.42 | 218.85 | 1.3320 | 40.189 | -24.81 | 0.7388 | 36.49 |
| | | Present[b] | 29.978 | 46.850 | 57.366 | 7.5590 | 21.398 | 1.216 | 0.5342 | 10.999 |
| | | Present[c] | 60.821 | 126.29 | 218.45 | 1.3587 | 40.097 | 1.053 | 0.7403 | 0.5938 |
| CLPT | 0.00 | Reference[a] | 60.822 | 126.30 | 218.49 | 1.3570 | 40.104 | 1.049 | 0.7391 | 0.5405 |
| | | Present | 60.822 | 126.30 | 218.49 | 1.3570 | 40.103 | 1.050 | 0.7401 | 0.5403 |

[a] (Kobayashi and Turvey, 1994)

[b] Based on the regular boundary condition for free edge

[c] Based on the modified boundary condition for free edge (see Remark 1)

### 5.3 Other plate shapes

To show the applicability and efficiency of the presented method, we have carried out the bending analysis of moderately thick plates with three other shapes: equilateral triangle, trapezoidal and skew plates of isotropic materials under uniformly distributed load with various boundary conditions. The presented results are compared to the numerical values obtained by the use of the differential cubature method based on FSDT (Liu and Liew, 1998a). The adopted non-dimensional values are the same as those in the studies by Liu and Liew (1998a). In all of the following problems, we have again used strategy H2 with the number of EBFs similar to the previous examples.

An isotropic plate having the shape of equilateral triangle with side length $a = 20\text{m}$ and thickness $h$ is shown in Figure 6. Total number of 60 boundary points and a grid of 21×18 points are selected as shown in Figs. 6.a and 6.b. The numerical results for the non-dimensional deflection $\bar{u}_3$, moment resultants $\bar{M}_{xx}$ and $\bar{M}_{yy}$ at the centroid point, obtained with the use of FSDT and CLPT, are reported in Table 12. These results include SSS, CCC and SCC boundary conditions with various thickness to span ratios. It is seen that the presented results obtained with FSDT are in good agreement with those given by Liu and Liew (1998a). The solution for a thin simply supported plate with the CLPT is also carried out and compared to the exact solution obtained by Timoshenko and Woinowsky-Krieger (1959). Again excellent agreement is seen between the results.

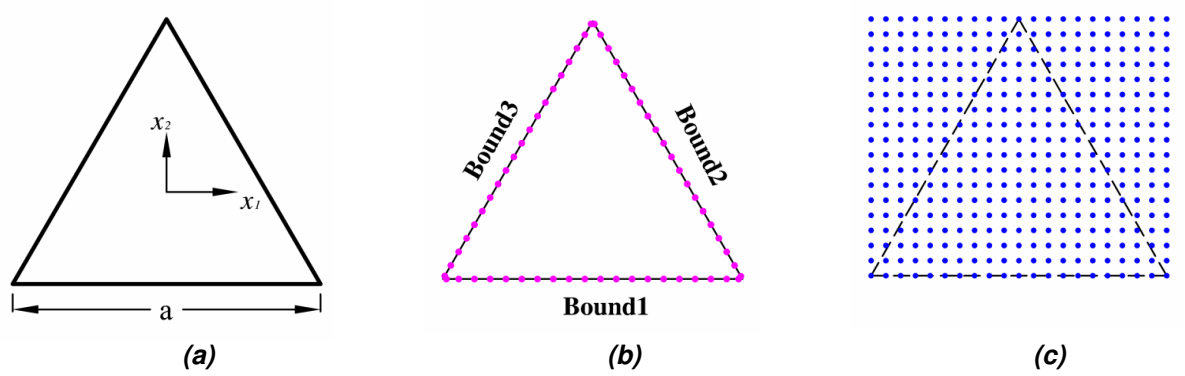


***Figure 6. The plate domain: (a) plate geometry; (b) Boundary points and sequence of boundary edges numbering; (c) Distribution of domain points.***

**Table 12. Non-dimensional deflection and moment resultants at the centroid point of a uniformly loaded equilateral triangle plate of isotropic material with different boundary conditions**

| Boundary conditions | h/a | Method | $\bar{u}_3^{(1)}$ | $\bar{M}_{xx}^{(2)}$ | $\bar{M}_{yy}^{(2)}$ |
|---|---|---|---|---|---|
| SSS | 0.01 | Presnet-CLPT | 0.631944 | 0.180555 | 0.180556 |
| | | Presnet-FSDT | 0.632806 | 0.180554 | 0.180555 |
| | | Reference[a] | 0.6328 | 0.1806 | 0.1805 |
| | | Exact[b] | 0.6319 | 0.1806 | 0.1806 |
| | 0.10 | Presnet-FSDT | 0.718612 | 0.180555 | 0.180556 |
| | | Reference[a] | 0.7186 | 0.1806 | 0.1806 |
| | 0.20 | Presnet-FSDT | 0.978611 | 0.180553 | 0.180556 |
| | | Reference[a] | 0.9800 | 0.1807 | 0.1808 |
| CCC | 0.10 | Presnet-FSDT | 0.278663 | 0.840536 | 0.840536 |
| | | Reference[a] | 0.2790 | 0.8403 | 0.8410 |
| | 0.25 | Presnet-FSDT | 0.747058 | 0.87526 | 0.87527 |
| | | Reference[a] | 0.7469 | 0.8754 | 0.8750 |
| SCC | 0.10 | Presnet-FSDT | 0.362373 | 0.106184 | 0.0988363 |
| | | Reference[a] | 0.3624 | 0.1062 | 0.0987 |
| | 0.25 | Presnet-FSDT | 0.868145 | 0.105755 | 0.121771 |
| | | Reference[a] | 0.8677 | 0.1057 | 0.1217 |

(1) $10^{-2}qa^4/(Eh^3)$; (2) $10^{-1}qa^2$;

[a] (Liu and Liew, 1998a); [b] (Timoshenko and Woinowsky-Krieger, 1959);

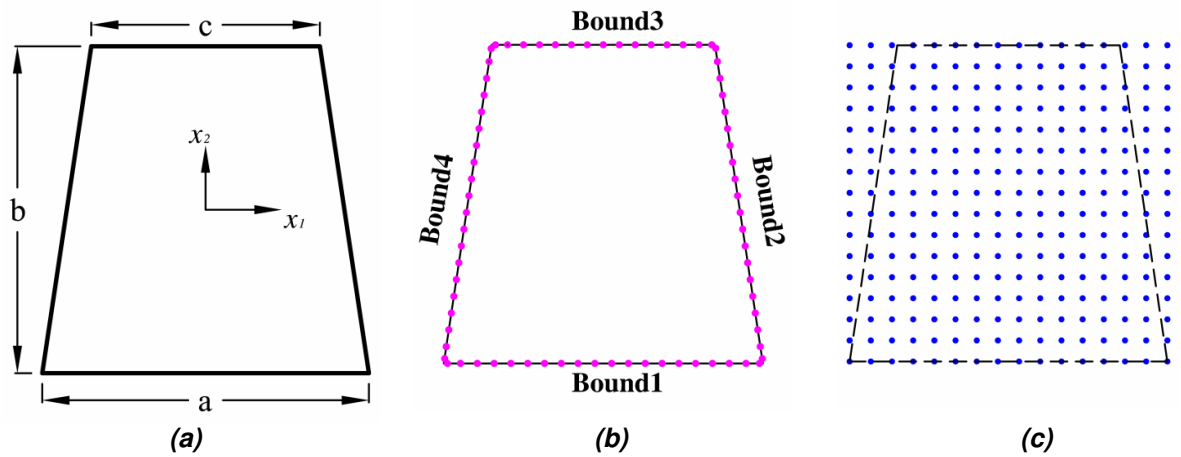


***Figure 7. The plate domain: (a) plate geometry; (b) Boundary points and sequence of boundary edges numbering; (c) Distribution of domain points.***

Table 13 includes the non-dimensional central deflection, moments and shear forces of an isotropic fully clamped trapezoidal plate with $b/a=1$ and $c/a=0.7$, (see Figure 7.a). The boundary points and the grid points of the domain are shown in Figure 7.b and 7.c, respectively. It can be observed that, again, the three sets are in excellent agreement, especially for the central deflections and moments.

**Table 13. Non-dimensional central deflections, moments and shear forces for a uniformly loaded trapezoidal isotropic plate with CCCC boundary condition** $(a/b=1.0, c/a=0.7)$ **.**

| h/a | Method | $\bar{u}_3^{(1)}$ | $\bar{M}_{xx}^{(2)}$ | $\bar{M}_{yy}^{(2)}$ | $\bar{M}_{xy}^{(2)}$ | $\bar{Q}_x^{(3)}$ | $\bar{Q}_y^{(3)}$ |
|---|---|---|---|---|---|---|---|
| 0.01 | Present-CLPT | 0.0856 | 0.2087 | 0.1634 | 0.0000 | 0.0000 | 0.7746 |
| | Present-FSDT | 0.0858 | 0.2087 | 0.1634 | 0.0000 | 0.0000 | 0.7747 |
| | Reference[a] | 0.0860 | 0.2090 | 0.1634 | 0.0000 | 0.0000 | 0.7758 |
| 0.10 | Presnet-FSDT | 0.1054 | 0.2100 | 0.1677 | 0.0000 | 0.0000 | 0.7925 |
| | Reference[a] | 0.1054 | 0.2100 | 0.1678 | 0.0000 | 0.0000 | 0.7923 |
| 0.15 | Presnet-FSDT | 0.1287 | 0.2103 | 0.1714 | 0.0000 | 0.0000 | 0.8164 |
| | Reference[a] | 0.1288 | 0.2104 | 0.1714 | 0.0000 | 0.0000 | 0.8115 |
| 0.20 | Presnet-FSDT | 0.1606 | 0.2101 | 0.1750 | 0.0000 | 0.0000 | 0.8400 |
| | Reference[a] | 0.1606 | 0.2102 | 0.1750 | 0.0000 | 0.0000 | 0.8367 |

(1) $10^{-2}qa^4/D$ ; (2) $10^{-1}qa^2$ ; (3) $10^{-2}qa$ ;

[a] (Liu and Liew, 1998a);

For the final example a skew rhombic plate with the side length $a$ and skew angle $\psi$ as shown in Figure 8 is considered. The non-dimensional deflection, maximum and minimum moments at the centroid point of the plate with $h/a=0.01$ for fully clamped and simply supported skew plates are presented in Table 14 and 15 respectively. The numerical results due to (Sengupta, 1995), in which a finite element method based on Mindlin's plate theory is used, are also reported in these tables for comparison.

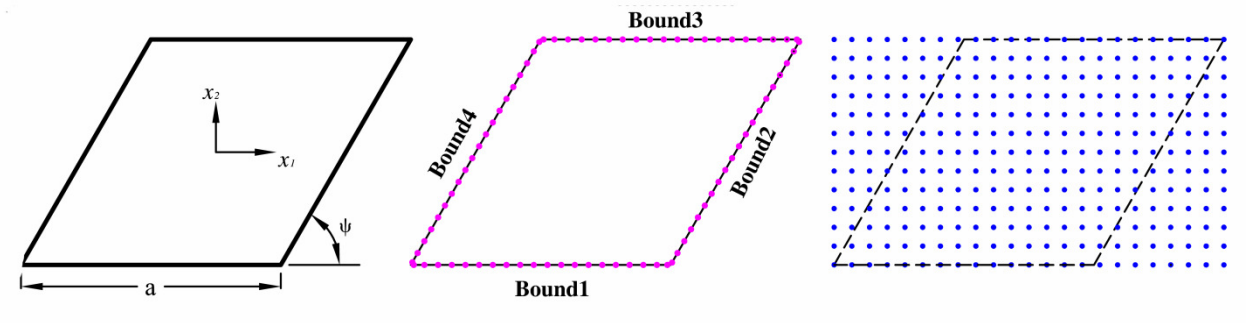


***(a)*** ***(b)*** ***(c)***

***Figure 8. The plate domain: (a) plate geometry; (b) Boundary points and sequence of boundary edges numbering; (c) Distribution of domain points.***

It is seen from Table 14 that the number of EBFs adopted is adequate enough to achieve close agreement with the reference values for a fully clamped plate. On the other hand, for a simply supported plate (Table 15), we have increased the number of EBFs by taking $\bar{M}=\bar{N}=4$ in order to accurately satisfy the boundary conditions. As pointed out by Liu and Liew (1998a), this might be the result of the singularity of stresses at the obtuse corners of the plate with skew angle smaller than $45^o$.

**Table 14. Non-dimensional deflections, maximum and minimum bending moments at the centroid of a uniformly loaded skew rhombic plate of isotropic material with CCCC boundary condition** $(h/a = 0.01)$**.**

| Skew angle (ψ) | Method | $(\bar{u}_3)_c^{(1)}$ | $(\bar{M}_c)_{\max}^{(2)}$ | $(\bar{M}_c)_{\min}^{(2)}$ |
|---|---|---|---|---|
| 75° | Present-CLPT | 1.7967 | 9.1192 | 8.0860 |
| | Present-FSDT | 1.8004 | 9.1209 | 8.0875 |
| | Reference[a] | 1.8017 | 9.1250 | 8.0930 |
| | Reference[b] | 1.8004 | 9.1257 | 8.0855 |
| 60° | Present-CLPT | 1.2 04 | 7.9139 | 6.1765 |
| | Present-FSDT | 1.2335 | 7.9156 | 6.1776 |
| | Reference[a] | 1.2332 | 7.9201 | 6.1729 |
| | Reference[b] | 1.2335 | 7.9161 | 6.1754 |
| 45° | Present-CLPT | 0.6037 | 5.7736 | 3.9095 |
| | Present-FSDT | 0.6058 | 5.7748 | 3.9103 |
| | Reference[a] | 0.6018 | 5.7800 | 3.8680 |
| | Reference[b] | 0.6051 | 5.7756 | 3.9003 |
| 30° | Present-CLPT | 0.1746 | 3.2166 | 1.8412 |
| | Present-FSDT | 0.1761 | 3.2177 | 1.8475 |
| | Reference[a] | 0.1715 | 3.2142 | 1.7208 |
| | Reference[b] | 0.1743 | 3.2089 | 1.8205 |

(1) $qa^4/(1600D)$; (2) $qa^2/400$;

[a] (Liu and Liew, 1998a); [b] (Sengupta, 1995);

**Table 15. Non-dimensional deflections, maximum and minimum bending moments at the centroid of a uniformly loaded skew rhombic plate of isotropic material with SSSS boundary condition** $(h/a = 0.01)$**.**

| Skew angle (ψ) | Method | $(\bar{u}_3)_c^{(1)}$ | $(\bar{M}_c)_{\max}^{(2)}$ | $(\bar{M}_c)_{\min}^{(2)}$ |
|---|---|---|---|---|
| 75° | Present-CLPT | 5.7838 | 19.1132 | 16.9438 |
| | Present-FSDT | 5.8032 | 1.9152 | 1.6983 |
| | Reference[a] | 5.7341 | 1.9061 | 1.6741 |
| | Reference[b] | 5.8468 | 1.9241 | 1.7097 |
| 60° | Present-CLPT | 3 7545 | 1.60416 | 1.2310 |
| | Present-FSDT | 3.8953 | 1.6470 | 1.2680 |
| | Reference[a] | 3.7591 | 1.6492 | 1.2418 |
| | Reference[b] | 4.1123 | 1.7075 | 1.3391 |
| 45° | Present-CLPT | 1.6154 | 1.0753 | 0.6856 |
| | Present-FSDT | 1.7296 | 1.1323 | 0.7180 |
| | Reference[a] | 1.8528 | 1.1988 | 0.7431 |
| | Reference[b] | 2.1330 | 1.2995 | 0.8866 |
| 30° | Present-CLPT | 0.5270 | 0.6520 | 0.3536 |
| | Present-FSDT | 0.5298 | 0.6593 | 0.3438 |
| | Reference[a] | 0.5449 | 0.6799 | 0.3321 |
| | Reference[b] | 0.6690 | 0.7734 | 0.4481 |

(1) $qa^4/(1600D)$; (2) $qa^2/40$;

[a] (Liu and Liew, 1998a); [b] (Sengupta, 1995);

## 6. CONCLUSIONS

In this report, we have employed a mesh-free approach for the bending analysis of laminated plates based on CLPT, FSDT and TSDT. In this method, the approximation function is a series of EBFs with unknown constant coefficients that can satisfy the governing partial differential equations. Imposition of the boundary conditions is performed through a collocation method on a set of scattered boundary points. Upon imposing the boundary conditions, the unknown coefficients of the approximation series are obtained with the aid of a transformation technique, which makes it possible to satisfy both the essential and natural boundary conditions simultaneously. The particular part is also solved using another set of EBFs. The associated boundary values of the particular solution are used to construct a modified form of the boundary conditions that should be imposed along the plate edges instead of the real values of the boundary conditions.

Numerical results for static analysis of square cross-ply laminated plates with two types of loading and various boundary conditions have been presented and compared to those available in the literature to verify the accuracy and efficiency of the present method. It should be noted that the application of the proposed method is not limited by the stacking sequence of the laminates.

In comparison with square or rectangular plates, the numerical results for laminated plates with other shapes are rare in the literature. Therefore, we have examined the bending problem of isotropic plates with annular sector, triangular, trapezoidal and rhombic configurations to validate the performance of the present method. It has been observed that the method can perform excellently in a wide range of problems defined for the bending analysis of laminated plates based on various plate theories.

## Appendix A

### Coefficients $L_{ij}$ for CLPT

$$
\begin{aligned}
L_{11} &= A_{11}d_1^2 + 2A_{16}d_1d_2 + A_{66}d_2^2,\\
L_{12} &= A_{16}d_1^2 + (A_{66} + A_{12})\, d_1d_2 + A_{26}d_2^2,\\
L_{13} &= -B_{11}d_1^3 - 3B_{16}d_1^2d_2 - (2B_{66} + B_{12})\, d_1d_2^2 - B_{26}d_2^3,\\
L_{22} &= A_{66}d_1^2 + 2A_{26}d_1d_2 + A_{22}d_2^2,\\
L_{23} &= -B_{22}d_2^3 - 3B_{26}d_1d_2^2 - (2B_{66} + B_{12})\, d_1^2d_2 - B_{16}d_1^3,
\end{aligned}
\tag{A.1}
$$

$$
L_{33} = D_{11}d_1^4 + 4D_{16}d_1^3d_2 + (2D_{12} + 4D_{66})d_1^2d_2^2 + 4D_{26}d_1d_2^3 + D_{22}\, d_2^4.
$$

### Coefficients $L_{ij}$ for FSDT

$$
\begin{aligned}
L_{11} &= A_{11}d_1^2 + 2A_{16}d_1d_2 + A_{66}d_2^2,\\
L_{12} &= A_{16}d_1^2 + (A_{66} + A_{12})\, d_1d_2 + A_{26}d_2^2,
\end{aligned}
$$

$$
\begin{aligned}
L_{13} &= 0,\\
L_{14} &= B_{11}d_1^2 + 2B_{16}d_1d_2 + B_{66}d_2^2,\\
L_{15} &= B_{16}d_1^2 + (B_{66} + B_{12})\ d_1d_2 + B_{26}d_2^2,\\
L_{22} &= A_{66}d_1^2 + 2A_{26}d_1d_2 + A_{22}d_2^2,\\
L_{23} &= 0,\\
L_{24} &= L_{15},\\
L_{25} &= B_{66}d_1^2 + 2B_{26}d_1d_2 + B_{22}d_2^2,\\
L_{33} &= -k_s\ (A_{55}d_1^2 + 2A_{45}d_1d_2 + A_{44}d_2^2),\\
L_{34} &= -k_s\ (A_{55}d_1 + A_{45}d_2),\\
L_{35} &= -k_s\ (A_{44}d_2 + A_{45}d_1),\\
L_{44} &= D_{11}d_1^2 + 2D_{16}d_1d_2 + D_{66}d_2^2 - k_sA_{55},\\
L_{45} &= D_{16}d_1^2 + (D_{66} + D_{12})\ d_1d_2 + D_{26}d_2^2 - k_sA_{45},\\
L_{55} &= D_{66}d_1^2 + 2D_{26}d_1d_2 + D_{22}\ d_2^2 - k_sA_{44}.
\end{aligned}
\tag{A.2}
$$

**Coefficients $L_{ij}$ for TSDT**

$$
\begin{aligned}
L_{11} &= A_{11}d_1^2 + 2A_{16}d_1d_2 + A_{66}d_2^2,\\
L_{12} &= A_{16}d_1^2 + (A_{66} + A_{12})\ d_1d_2 + A_{26}d_2^2,\\
L_{13} &= -C_1\ (E_{11}d_1^3 + 3E_{16}d_1^2d_2 + (E_{12} + 2E_{66})\ d_1d_2^2 + E_{26}d_2^3),\\
L_{14} &= (B_{11} - C_1\ E_{11})\ d_1^2 + 2(B_{16} - C_1\ E_{16})\ d_1d_2 + (B_{66} - C_1\ E_{66})\ d_2^2,\\
L_{15} &= (B_{16} - C_1\ E_{16})\ d_1^2 + (B_{66} + B_{12} - C_1\ (E_{66} + E_{12}))\ d_1d_2 + (B_{26} - C_1\ E_{26})\ d_2^2,\\
L_{22} &= A_{66}d_1^2 + 2A_{26}d_1d_2 + A_{22}d_2^2,\\
L_{23} &= -C_1\ (E_{16}d_1^3 + 3E_{26}d_1d_2^2 + (E_{12} + 2E_{66})\ d_1^2d_2 + E_{22}d_2^3),\\
L_{24} &= L_{15},\\
L_{25} &= (B_{66} - C_1\ E_{66})\ d_1^2 + 2(B_{26} - C_1\ E_{26})\ d_1d_2 + (B_{22} - C_1\ E_{22})\ d_2^2,\\
L_{33} &= -(A_{55} - 2\ C_2\ D_{55} + C_2^2\ F_{55})\ d_1^2 - 2(A_{45} - 2\ C_2\ D_{45} + C_2^2\ F_{45})\ d_1d_2\\
&\quad - (A_{44} - 2\ C_2\ D_{44} + C_2^2\ F_{44})\ d_2^2 + C_1^2(H_{11}d_1^4 + (2H_{12} + 4H_{66})\ d_1^2d_2^2 + 4H_{16}d_1^3d_2\\
&\quad + 4H_{26}d_1d_2^3 + H_{22}d_2^4),\\
L_{34} &= -(A_{55} - 2\ C_2\ D_{55} + C_2^2\ F_{55})\ d_1 - (A_{45} - 2\ C_2\ D_{45} + C_2^2\ F_{45})\ d_2 - C_1\ ((F_{11} - C_1\ H_{11})\ d_1^3 +\\
&\quad 3(F_{16} - C_1\ H_{16})\ d_1^2d_2 + (F_{12} + 2F_{66} - C_1\ (H_{12} + 2\ H_{66}))\ d_1d_2^2 + (F_{26} - C_1\ H_{26})\ d_2^3),\\
L_{35} &= -(A_{44} - 2\ C_2\ D_{44} + C_2^2\ F_{44})\ d_2 - (A_{45} - 2\ C_2\ D_{45} + C_2^2\ F_{45})\ d_1 - C_1\ ((F_{16} - C_1\ H_{16})\ d_1^3 +\\
&\quad (F_{12} + 2F_{66} - C_1\ (H_{12} + 2H_{66}))\ d_1^2d_2 + 3(F_{26} - C_1\ H_{26})\ d_1d_2^2 + (F_{22} - C_1\ H_{22})\ d_2^3),
\end{aligned}
$$

$$
\begin{aligned}
L_{44} &= (D_{11} - 2\,C_1\,F_{11} + C_1^2\,H_{11})\,d_1^2 + 2(D_{16} - 2\,C_1\,F_{16} + C_1^2\,H_{16})\,d_1 d_2 + \\
&\quad (D_{66} - 2\,C_1\,F_{66} + C_1^2\,H_{66})\,d_2^2 - (A_{55} - 2\,C_2\,D_{55} + C_2^2\,F_{55}), \\
L_{45} &= (D_{16} - 2\,C_1\,F_{16} + C_1^2\,H_{16})\,d_1^2 + (D_{66} + D_{12} - 2\,C_1\,(F_{66} + F_{12}) + C_1^2\,(H_{66} + H_{12}))\,d_1 d_2 + \\
&\quad (D_{26} - 2\,C_1\,F_{26} + C_1^2\,H_{26})\,d_2^2 - (A_{45} - 2\,C_2\,D_{45} + C_2^2\,F_{45}), \\
L_{55} &= (D_{66} - 2\,C_1\,F_{66} + C_1^2\,H_{66})\,d_1^2 + 2(D_{26} - 2\,C_1\,F_{26} + C_1^2\,H_{26})\,d_1 d_2 + \\
&\quad (D_{22} - 2\,C_1\,F_{22} + C_1^2\,H_{22})\,d_2^2 - (A_{44} - 2\,C_2\,D_{44} + C_2^2\,F_{44}),
\end{aligned}
\tag{A.3}
$$

where

$$
d_1^m = \frac{\partial^m(.)}{\partial x_1^m},\ d_2^m = \frac{\partial^m(.)}{\partial x_2^m},\ x_1 = x,\ x_2 = y \tag{A.4}
$$

## Appendix B

### Coefficients $B_{ij}$ for SS boundary in TSDT

$$
\begin{aligned}
&B_{1i}^{\mathrm{SS}} = s_i,\ \ B_{13}^{\mathrm{SS}} = B_{1(i+3)}^{\mathrm{SS}} = 0 \\
&B_{2i}^{\mathrm{SS}} = n_k\,n_l\,A_{klij}\,d_j \\
&B_{23}^{\mathrm{SS}} = -C_1 n_k\,n_l\,E_{klij}\,d_i\,d_j \\
&B_{2(i+3)}^{\mathrm{SS}} = n_k\,n_l\,(B_{klij} - C_1 E_{klij})\,d_j \\
&B_{3i}^{\mathrm{SS}} = 0,\quad B_{33}^{\mathrm{SS}} = 1,\quad B_{3(3+i)}^{\mathrm{SS}} = 0 \\
&B_{4i}^{\mathrm{SS}} = n_k\,n_l\,E_{klij}\,d_j \\
&B_{43}^{\mathrm{SS}} = -C_1 n_k\,n_l\,H_{klij}\,d_i\,d_j \\
&B_{4(i+3)}^{\mathrm{SS}} = n_k\,n_l\,(F_{klij} - C_1 H_{klij})\,d_j \\
&B_{5i}^{\mathrm{SS}} = 0,\ \ B_{53}^{\mathrm{SS}} = 0,\ \ B_{5(i+3)}^{\mathrm{SS}} = s_i \\
&B_{6i}^{\mathrm{SS}} = n_k\,n_l\,B_{klij}\,d_j - C_1 B_{4i}^{\mathrm{SS}} \\
&B_{63}^{\mathrm{SS}} = -C_1 n_k\,n_l\,F_{klij}\,d_i\,d_j - C_1 B_{43}^{\mathrm{SS}} \\
&B_{6(i+3)}^{\mathrm{SS}} = n_k\,n_l\,(D_{klij} - C_1 F_{klij})\,d_j - C_1 B_{4(i+3)}^{\mathrm{SS}}
\end{aligned}
\tag{B.1}
$$

### Coefficients $B_{ij}$ for C boundary in TSDT

$$
\begin{aligned}
&B_{1i}^{\mathrm{C}} = s_i,\ \ B_{13}^{\mathrm{C}} = B_{1(i+3)}^{\mathrm{C}} = 0 \\
&B_{2i}^{\mathrm{C}} = n_i,\ \ B_{23}^{\mathrm{C}} = B_{2(i+3)}^{\mathrm{C}} = 0
\end{aligned}
$$

$$
\begin{aligned}
&B_{3i}^{\mathrm{C}}=0,\quad B_{33}^{\mathrm{C}}=1,\quad B_{3(3+i)}^{\mathrm{C}}=0\\
&B_{4i}^{\mathrm{C}}=n_i d_i,\quad B_{43}^{\mathrm{C}}=B_{4(i+3)}^{\mathrm{C}}=0\\
&B_{5i}^{\mathrm{C}}=0,\quad B_{53}^{\mathrm{C}}=0,\quad B_{5(i+3)}^{\mathrm{C}}=s_i\\
&B_{6i}^{\mathrm{C}}=0,\quad B_{63}^{\mathrm{C}}=0,\quad B_{6(i+3)}^{\mathrm{C}}=n_i
\end{aligned}
\tag{B.2}
$$

**Coefficients $B_{ij}$ for F boundary in TSDT**

$$
\begin{aligned}
&B_{1i}^{\mathrm{F}}=n_k s_l A_{klij} d_j,\\
&B_{13}^{\mathrm{F}}=-C_1 n_k s_l E_{klij} d_i d_j\\
&B_{1(i+3)}^{\mathrm{F}}=n_k s_l (B_{klij}-C_1 E_{klij}) d_j\\
&B_{2\gamma}^{\mathrm{F}}=B_{2\gamma}^{\mathrm{SS}},\quad \gamma=\overline{1,5}\\
&B_{3i}^{\mathrm{F}}=C_1 n_k E_{klij} d_j d_l\\
&B_{33}^{\mathrm{F}}=-C_1^2 n_k H_{klij} d_i d_j d_l+n_k (A_{k3i3}-2C_2 D_{k3i3}+C_2^2 F_{k3i3}) d_i\\
&B_{3(i+3)}^{\mathrm{F}}=C_1 n_k (F_{klij}-C_1 H_{klij}) d_j d_l+n_k (A_{k3i3}-2C_2 D_{k3i3}+C_2^2 F_{k3i3})\\
&B_{4\gamma}^{\mathrm{F}}=B_{4\gamma}^{\mathrm{SS}},\quad \gamma=\overline{1,5}\\
&B_{5i}^{\mathrm{F}}=n_k s_l B_{klij} d_j-C_1 B_{4i}^{\mathrm{F}}\\
&B_{53}^{\mathrm{F}}=-C_1 n_k s_l F_{klij} d_i d_j-C_1 B_{43}^{\mathrm{F}}\\
&B_{5(i+3)}^{\mathrm{F}}=n_k s_l (D_{klij}-C_1 F_{klij}) d_j-C_1 B_{4(i+3)}^{\mathrm{F}}\\
&B_{6\gamma}^{\mathrm{F}}=B_{6\gamma}^{\mathrm{SS}},\quad \gamma=\overline{1,5}
\end{aligned}
\tag{B.3}
$$

**Coefficients $B_{ij}$ for G boundary in TSDT**

$$
\begin{aligned}
&B_{1\gamma}^{\mathrm{G}}=B_{1\gamma}^{\mathrm{F}},\quad B_{2\gamma}^{\mathrm{G}}=B_{2\gamma}^{\mathrm{C}},\quad B_{3\gamma}^{\mathrm{G}}=B_{3\gamma}^{\mathrm{F}}\\
&B_{4\gamma}^{\mathrm{G}}=B_{4\gamma}^{\mathrm{C}},\quad B_{5\gamma}^{\mathrm{G}}=B_{5\gamma}^{\mathrm{F}},\quad B_{6\gamma}^{\mathrm{G}}=B_{6\gamma}^{\mathrm{C}},\quad \gamma=\overline{1,5}
\end{aligned}
\tag{B.4}
$$

**Coefficients $B_{ij}$ for SS boundary in FSDT**

$$
\begin{aligned}
&B_{1i}^{\mathrm{SS}}=s_i,\quad B_{13}^{\mathrm{SS}}=B_{1(i+3)}^{\mathrm{SS}}=0\\
&B_{2i}^{\mathrm{SS}}=n_k n_l A_{klij} d_j,\quad B_{23}^{\mathrm{SS}}=0,\quad B_{2(i+3)}^{\mathrm{SS}}=n_k n_l B_{klij} d_j\\
&B_{3i}^{\mathrm{SS}}=0,\quad B_{33}^{\mathrm{SS}}=1,\quad B_{3(3+i)}^{\mathrm{SS}}=0\\
&B_{4i}^{\mathrm{SS}}=0,\quad B_{43}^{\mathrm{SS}}=0,\quad B_{4(i+3)}^{\mathrm{SS}}=s_i\\
&B_{5i}^{\mathrm{SS}}=n_k n_l B_{klij} d_j,\quad B_{53}^{\mathrm{SS}}=0,\quad B_{5(i+3)}^{\mathrm{SS}}=n_k n_l D_{klij} d_j
\end{aligned}
\tag{B.5}
$$

**Coefficients $B_{ij}$ for C boundary in FSDT**

$$
\begin{aligned}
&B_{1i}^{\mathrm{C}} = s_i, \quad B_{13}^{\mathrm{C}} = B_{1(i+3)}^{\mathrm{C}} = 0 \\
&B_{2i}^{\mathrm{C}} = n_i, \quad B_{23}^{\mathrm{C}} = B_{2(i+3)}^{\mathrm{C}} = 0 \\
&B_{3i}^{\mathrm{C}} = 0, \quad B_{33}^{\mathrm{C}} = 1, \quad B_{3(3+i)}^{\mathrm{C}} = 0 \\
&B_{4i}^{\mathrm{C}} = 0, \quad B_{43}^{\mathrm{C}} = 0, \quad B_{4(i+3)}^{\mathrm{C}} = s_i \\
&B_{5i}^{\mathrm{C}} = B_{53}^{\mathrm{C}} = 0, \quad B_{5(i+3)}^{\mathrm{C}} = n_i
\end{aligned}
\tag{B.6}
$$

**Coefficients $B_{ij}$ for F boundary in FSDT**

$$
\begin{aligned}
&B_{1i}^{\mathrm{F}} = n_k s_l A_{klij} d_j, \quad B_{13}^{\mathrm{F}} = 0, \quad B_{1(i+3)}^{\mathrm{F}} = n_k s_l B_{klij} d_j \\
&B_{2\gamma}^{\mathrm{F}} = B_{2\gamma}^{\mathrm{SS}}, \quad \gamma = \overline{1,5} \\
&B_{3i}^{\mathrm{F}} = 0, \quad B_{33}^{\mathrm{F}} = n_k k_s A_{k\,3i\,3} d_i, \quad B_{3(i+3)}^{\mathrm{F}} = n_k k_s A_{k\,3i\,3} \\
&B_{4i}^{\mathrm{F}} = n_k s_l B_{klij} d_j, \quad B_{43}^{\mathrm{F}} = 0, \\
&B_{4(i+3)}^{\mathrm{F}} = n_k s_l D_{klij} d_j \\
&B_{5\gamma}^{\mathrm{F}} = B_{5\gamma}^{\mathrm{SS}}, \quad \gamma = \overline{1,5}
\end{aligned}
\tag{B.7}
$$

**Coefficients $B_{ij}$ for G boundary in FSDT**

$$
\begin{aligned}
&B_{1\gamma}^{\mathrm{G}} = B_{1\gamma}^{\mathrm{F}}, \quad B_{2\gamma}^{\mathrm{G}} = B_{2\gamma}^{\mathrm{C}}, \quad B_{3\gamma}^{\mathrm{G}} = B_{3\gamma}^{\mathrm{F}} \\
&B_{4\gamma}^{\mathrm{G}} = B_{4\gamma}^{\mathrm{C}}, \quad B_{5\gamma}^{\mathrm{G}} = B_{5\gamma}^{\mathrm{F}}, \quad \gamma = \overline{1,5}
\end{aligned}
\tag{B.8}
$$

**Coefficients $B_{ij}$ for SS boundary in CLPT**

$$
\begin{aligned}
&B_{1i}^{\mathrm{SS}} = s_i, \quad B_{13}^{\mathrm{SS}} = 0 \\
&B_{2i}^{\mathrm{SS}} = n_k n_l A_{klij} d_j, \quad B_{23}^{\mathrm{SS}} = -n_k n_l B_{klij} d_i d_j \\
&B_{3i}^{\mathrm{SS}} = 0, \quad B_{33}^{\mathrm{SS}} = 1 \\
&B_{4i}^{\mathrm{SS}} = n_k n_l B_{klij} d_j, \quad B_{43}^{\mathrm{SS}} = -n_k n_l D_{klij} d_i d_j
\end{aligned}
\tag{B.9}
$$

**Coefficients $B_{ij}$ for C boundary in CLPT**

$$
\begin{aligned}
&B_{1i}^{\mathrm{C}} = s_i, \quad B_{13}^{\mathrm{C}} = 0 \\
&B_{2i}^{\mathrm{C}} = n_i, \quad B_{23}^{\mathrm{C}} = 0 \\
&B_{3i}^{\mathrm{C}} = 0, \quad B_{33}^{\mathrm{C}} = 1
\end{aligned}
$$

$$B_{4i}^{\mathrm{C}} = 0, \quad B_{43}^{\mathrm{C}} = n_i d_i \tag{B.10}$$

**Coefficients $B_{ij}$ for F boundary in CLPT**

$$\begin{aligned}
&B_{1i}^{F} = n_k s_l A_{klij} d_j, \quad B_{13}^{F} = -n_k s_l B_{klij} d_i d_j \\
&B_{2i}^{F} = n_k n_l A_{klij} d_j, \quad B_{23}^{F} = -n_k n_l B_{klij} d_i d_j \\
&B_{3i}^{F} = n_k B_{klij} d_j d_l + \partial(n_k s_l B_{klij} d_j)/\partial s \\
&B_{33}^{F} = -n_k D_{klij} d_i d_j d_l - \partial(n_k s_l D_{klij} d_i d_j)/\partial s \\
&B_{4i}^{F} = n_k n_l B_{klij} d_j, \quad B_{43}^{F} = -n_k n_l D_{klij} d_i d_j
\end{aligned} \tag{B.11}$$

**Coefficients $B_{ij}$ for G boundary in CLPT**

$$\begin{aligned}
&B_{1\gamma}^{\mathrm{G}} = B_{1\gamma}^{\mathrm{F}}, \quad B_{2\gamma}^{\mathrm{G}} = B_{2\gamma}^{\mathrm{C}}, \\
&B_{3\gamma}^{\mathrm{G}} = B_{3\gamma}^{\mathrm{F}}, \quad B_{4\gamma}^{\mathrm{G}} = B_{4\gamma}^{\mathrm{C}}, \qquad \gamma = \overline{1,3}
\end{aligned} \tag{B.12}$$

in the above indicial notations

$$\begin{aligned}
&i, j, k, l = \overline{1,2} \\
&d_i = \frac{\partial(.)}{\partial x_i} \ (\mathrm{i}=\overline{1,2}), \quad x_1 \leftrightarrow x, \ \mathrm{x}_2 \leftrightarrow y \\
&n_1 \leftrightarrow n_x, \ n_2 \leftrightarrow n_x, \ \ s_1 \leftrightarrow s_x, \ s_2 \leftrightarrow s_y
\end{aligned} \tag{B.13}$$

The stiffness components, expressed in the double indexed system, can be related to their corresponding ones in the single indexed system as follows

$$11 \equiv 1, \quad 22 \equiv 2, \quad 12 \text{ or } 21 \equiv 6, \quad 13 \text{ or } 31 \equiv 5, \quad 23 \text{ or } 32 \equiv 4 \tag{B.14}$$

## References


Akhras, G., Li, W., 2005. Static and free vibration analysis of composite plates using spline finite strips with higher-order shear deformation. Composites Part B 36, 496-503.

Atluri, S.N., Zhu, T., 1998. A new meshless local Petrov-Galerkin (MLPG) approach in computational mechanics. Comput. Mech. 22, 117-127.

Belinha, J., Dinis, L., 2006. Analysis of plates and laminates using the element-free Galerkin method. Comput. Struct. 84, 1547-1559.

Belytschko, T., Lu, Y.Y., Gu, L., 1994. Element-free Galerkin methods. Int. J. Numer. Methods Eng. 37, 229-256.

Boroomand, B., Mossaiby, F., 2005a. Generalization of robustness test procedure for error estimators. Part I: formulation for patches near kinked boundaries. Int. J. Numer. Methods Eng. 64, 427–460.

Boroomand, B., Mossaiby, F., 2005b. Generalization of robustness test procedure for error estimators. Part II: test results for error estimators using SPR and REP. Int. J. Numer. Methods Eng. 64, 461–502.

Boroomand, B., Mossaiby, F., 2006. Dynamic solution of unbounded domains using finite element method: Discrete Green's functions in frequency domain. Int. J. Numer. Methods Eng. 67, 1491–1530.

Boroomand, B., Soghrati, S., Movahedian, B., 2009. Exponential basis functions in solution of static and time harmonic elastic problems in a meshless style. Int. J. Numer. Methods Eng. 81, 971-1018.

De Barcellos, C.S., Westphal, J.T., 1992. Reissner/Mindlin's plate models and the boundary element method in: MS, I. (Ed.), Seventh Conference on Boundary Element Technology Computational Mechanics Brebbia CA. pp. 589-604.

Dong, C.Y., Lo, S.H., Cheung, Y.K., Lee, K.Y., 2004. Anisotropic thin plate bending problem by Trefftz boundary collocation method. Eng. Anal. Boundary Elem. 28, 1017–1024.

Dong, Y.F., Defreitas, J.A.T., 1994. A quadrilateral hybrid stress element for Mindlin plates based on incompatible displacements. Int. J. Numer. Methods Eng. 37, 279-296.

Donning, B.M., Liu, W.K., 1998. Meshless methods for shear-deformable beams and plates. Comput. Meth. Appl. Mech. Eng. 152, 47-71.

Duarte, C.A., Oden, J.T., 1996. An h-p adaptive method using clouds. Comput. Meth. Appl. Mech. Eng. 139, 237-262.

Garcia, O.A., Fancello, E.A., de Barcellos, C.S., Duarte, C.A., 2000. HP-Clouds in Mindlin's thick plate model. Int. J. Numer. Methods Eng. 47, 1381-1400.

Jirousek, J., Guex, L., 1986. The hybrid-Trefftz finite element model and its application to plate bending. Int. J. Numer. Methods Eng. 23, 651-693.

Jirousek, J., Leon, N., 1977. A powerful finite element element for plate blending. Comput. Meth. Appl. Mech. Eng. 12, 77-96.

Katsikadelis, J.T., Yotis, A.J., 1993. A new boundary element solution of thick plates modelled by Reissner's theory. Eng. Anal. Boundary Elem. 12, 65-74.

Khdeir, A.A., Reddy, J.N., 1991. Analytical solutions of refined plate theories of cross-ply composite laminates. J. Pressure Vessel Technol. 113, 570-578.

Khdeir, A.A., Reddy, J.N., Librescu, L., 1987. Analytical solution of a refined shear deformation theory for rectangular composite plates. Int. J. Solids Struct. 23, 1447-1463.

Kirchhoff, G., 1850. Uber das gleichgewicht und die bewegung einer elatischen scheibl. Mathematik 40, 51-88.

Kobayashi, H., Turvey, G.J., 1994. Elastic small deflection analysis of annular sector Mindlin plates. Int. J. Mech. Sci. 36, 811-827.

Kocak, S., Hassis, H., 2003. A higher order shear deformable finite element for homogeneous plates. Eng. Struct. 25, 131-139.

Kupradze, V.D., Aleksidze, M.A., 1964. The method of functional equations for the approximate solution of certain boundary value problems. USSR Comput. Math. Math. Phys. 4, 82–126.

Levinson, M., 1980. An accurate, simple theory for statics and dynamics of elastic plates. Mech. Res. Commun. 7, 343-350.

Li, Z.C., Lu, T.T., Huang, H.T., Cheng, A.H.D., 2007. Trefftz, collocation, and other boundary methods—A comparison. Numer. Methods Partial Differ. Equ. 23, 93–144.

Liew, K.M., Han, J.B., 1997. A four-node differential quadrature method for straight-sided quadrilateral Reissner/Mindlin plates. Commun. Numer. Methods Eng. 13, 73-81.

Liu, F.L., Liew, K.M., 1998a. Differential cubature method for static solutions of arbitrarily shaped thick plates. Int. J. Solids Struct. 35, 3655-3674.

Liu, F.L., Liew, K.M., 1998b. Static analysis of Reissner-Mindlin plates by differential quadrature element method. ASME J. Appl. Mech. 65, 705-710.

Liu, L., Chua, L.P., Ghista, D.N., 2007. Mesh-free radial basis function method for static, free vibration and buckling analysis of shear deformable composite laminates. Compos. Struct. 78, 58-69.

Liu, W.K., Jun, S., Li, S., Adee, J., Belytschko, T., 1995. Reproducing kernel particle methods for structural dynamics. Int. J. Numer. Methods Eng. 38, 1655-1679.
Liu, Y., Li, R., 2010. Accurate bending analysis of rectangular plates with two adjacent edges free and the others clamped or simply supported based on new symplectic approach. Appl. Math. Modell. 34, 856-865.
Lo, K., Christensen, R., Wu, E., 1977. A high-order theory of plate deformation. ASME J. Appl. Mech. 44, 669-676.
Mindlin, R.D., 1951. Influence of rotatory inertia and shear on flexural motions of isotropic, elastic plates. J. Appl. Mech. 18, 31-38.
Nayroles, B., Touzot, G., Villon, P., 1991. The diffuse elements method. Comptes Rendus De L Academie Des Sciences Serie Ii 313, 133-138.
Oktem, A.S., Chaudhuri, R.A., 2007. Levy type analysis of cross-ply plates based on higher-order theory. Compos. Struct. 78, 243-253.
Pandya, B.N., Kant, T., 1988. Flexural analysis of laminated composites using refined higher-order C0 plate bending elements. Comput. Meth. Appl. Mech. Eng. 66, 173-198.
Reddy, J.N., 1984. A simple higher-order theory for laminated composite plates. ASME Journal of Applied Mechanics 51, 745-752.
Reddy, J.N., 2004. Mechanics of Laminated Composite Plates and Shells: Theory and Analysis CRC Press.
Sengupta, D., 1995. Performance study of a simple finite element in the analysis of skew rhombic plates. Comput. Struct. 54, 1173-1182.
Srinivas, S., Rao, A.K., 1970. Bending, vibration and buckling of simply supported thick orthotropic rectangular plates and laminates. Int. J. Solids Struct. 6, 1463-1481.
Swaminathan, K., Ragounadin, D., 2004. Analytical solutions using a higher-order refined theory for the static analysis of antisymmetric angle-ply composite and sandwich plates. Compos. Struct. 64, 405-417.
Timoshenko, S.P., Woinowsky-Krieger, S., 1959. Theory of plates and shells. McGraw-Hill, New York.
Wang, J., Liew, K.M., Tan, M.J., Rajendran, S., 2002. Analysis of rectangular laminated composite plates via FSDT meshless method. Int. J. Mech. Sci. 44, 1275-1293.
Wang, J.G., Liu, G.R., 2001. A point interpolation meshless method based on radial basis functions. Int. J. Numer. Methods Eng. 54, 1623-1648.
Whitney, J.M., Sun, C.T., 1974. A refined theory for laminated, anisotropic, cylindrical shells. J. Appl. Mech. 41, 471-476.
Yildiz, H., Sarikanat, M., 2001. Finite-element analysis of thick composite beams and plates. Compos. Sci. Technol. 61, 1723-1727.
Zhang, Y.X., Yang, C.H., 2009. Recent developments in finite element analysis for laminated composite plates. Compos. Struct. 88, 147-157.